

Giant magnetostriction

K. P. Belov, G. I. Kataev, R. Z. Levitin, S. A. Nikitin, and V. I. Sokolov

M. V. Lomonosov Moscow State University
Usp. Fiz. Nauk **140**, 271–313 (June 1983)

This review summarizes the results of studies of anisotropic magnetostriction in rare-earth and actinide magnetics. Experimental data are given on the magnetostrictive constants in the rare-earth metals, alloys, intermetallic compounds, garnet ferrites, various uranium compounds, etc. The nature of the giant magnetostriction observed in compounds of the rare earths and actinides is analyzed. This magnetostriction is shown in most cases to have a single-ion origin, and to be due to interaction of the orbital moment of the rare-earth (or actinide) ion with the crystal field of the lattice. The influence is discussed of the magnetoelastic interaction on the physical properties (magnetic anisotropy, elastic modulus, etc.) of rare-earth and actinide magnetics. The parameters of intermetallic compounds showing giant magnetostriction in the room-temperature region and the possibilities of technical application are discussed.

PACS numbers: 75.80. + q

TABLE OF CONTENTS

1. Introduction	518
2. On a phenomenological description of magnetostriction	519
3. Rare-earth and actinide magnetic materials with giant magnetostriction	519
a) Rare-earth metals and alloys. b) Intermetallic compounds of the rare earths. c) Garnet ferrites. d) Compounds of the actinides. e) Paramagnetic compounds of the rare earths.	
4. A theoretical model of giant magnetostriction	523
5. Studies of giant magnetostriction in rare-earth alloys and compounds	526
6. The effect of giant magnetostriction on the magnetic anisotropy and the elastic properties of rare-earth and actinide magnetic materials	533
7. Dynamic properties and possible applications of materials showing giant magnetostriction in technology	536
8. Conclusion	539
References	540

1. INTRODUCTION

The phenomenon of magnetostriction (change of dimensions of a magnetic material upon changing its magnetic state) was discovered by Joule more than 130 years ago.¹ Nevertheless it is attracting the attention of investigators up to the present. Primarily this involves the fact that magnetostriction governs not only the energy of magnetic anisotropy, but also the course of the technical magnetization curve (owing to the appearance of magnetoelastic anisotropy). In seeking new magnetic materials, one must have information on the magnetostrictive constants, as well as the magnetic anisotropy constants.²

Spontaneous magnetostriction, i.e., magnetostrictive deformation caused by a change in the magnetic state of an object upon cooling or heating, gives rise to bulk and elastic anomalies ("invar" and "elinvar" properties).^{3,4}

Moreover, the features of the course of magnetic phase transitions at Curie and Néel points depend on the character of the manifestation of spontaneous magnetostriction. First-order transitions arise at the Curie point under the influence of a large spontaneous magnetostriction instead of the usual second-order transitions.^{5,6} Moreover, in a number of materials spontaneous magnetostriction gives rise to a special type of magnetic phase transitions—magnetoorientational.⁷

Finally, studies of magnetostriction undoubtedly are of applied interest, since they offer a physical basis for designing sound generators,⁸ contactors, and translation drives in automation and optoelectronic systems.

For a long time magnetostriction was studied in metals, alloys, and compounds based on the iron-group elements. The relative elongation $\lambda = \Delta l/l$ in the technical saturation fields for polycrystalline specimens of iron and nickel at low temperatures and room temperature is small: $(25-35) \times 10^{-6}$. Somewhat larger values of the magnetostriction are observed in single crystals of these metals. In cobalt and its alloys (e.g., in permendur) and in cobalt ferrite, the magnetostriction is considerably larger, but as a rule it does not exceed 10^{-4} .

It was first established in 1961^{9,10} that the magnetostriction in the rare-earth metals terbium and dysprosium and also in their alloys and compounds at low temperatures exceeds the magnetostriction of metals and alloys based on the iron-group elements by factors of tens, hundreds, and in some cases thousands. It has been subsequently shown that the phenomenon of giant magnetostriction is observed in other rare-earth metals and their compounds, and also in a number of uranium and other actinide magnetic materials.^{11,12}

This review presents the results of experimental study of giant magnetostriction in various magnetic materials, analyzes the nature of this phenomenon and its

connection with the electronic structure of the rare-earth or actinide ion, examines the effect of giant magnetostriction on other properties of magnetic materials, and discusses the possible applications of giant magnetostriction in technology.

2. ON A PHENOMENOLOGICAL DESCRIPTION OF MAGNETOSTRICTION

The phenomenon of magnetostriction manifests the dependence of the magnetic and exchange interactions on the interatomic distances. The microscopic theory of magnetostriction has been sufficiently developed up to now; the existing theories are mainly phenomenological in nature.

Field-induced magnetostriction has been studied in greatest detail. This magnetostriction has several sources.

First there is the magnetostriction caused by the rotation of the magnetization vectors with respect to the crystal axes when the field direction does not coincide with the axis of easy magnetization of the crystal. Second there is the magnetostriction of a paraprocess, which arises from a change in the value of the spontaneous magnetization in fields above that for technical saturation.³ In most materials the magnetostriction of a paraprocess is small and isotropic in nature. In the rare-earth metals and their alloys, it is considerable in magnitude and is anisotropic. One can also single out magnetostriction caused by processes of domain-boundary displacement and magnetostriction caused by the magnetostatic interaction and associated with the shape of the specimen.

The relationships of magnetostrictive deformations to the direction of measurement and the orientation of the magnetization in crystals can be derived phenomenologically on the basis of the crystallographic symmetry. Without stopping to derive these formulas (see, e.g., Ref. 13), we shall present them for the crystal structures most frequently encountered in rare-earth compounds—hexagonal and cubic. If we restrict the expansion of the magnetoelastic component of the Hamiltonian in harmonic polynomials to terms quadratic in the direction cosines of the magnetization vector α_i , then the magnetostrictive deformation of a hexagonal crystal in the direction fixed by the direction cosines is described by the relationship

$$\lambda = \lambda_1^{\alpha,0} (\beta_x^2 + \beta_y^2) + \lambda_2^{\alpha,0} \beta_z^2 + \lambda_3^{\alpha,2} (\beta_x^2 + \beta_y^2) \left(\alpha_x^2 - \frac{1}{3} \right) + \lambda_4^{\alpha,2} \beta_z^2 \left(\alpha_x^2 - \frac{1}{3} \right) - \lambda_5^{\alpha,2} \left[\frac{1}{2} (\beta_x^2 - \beta_y^2) (\alpha_x^2 - \alpha_y^2) + 2\beta_x \beta_y \alpha_x \alpha_y \right] + 2\lambda_6^{\alpha,2} (\beta_x \alpha_x + \beta_y \alpha_y) \beta_z \alpha_z. \quad (1)$$

The first two terms in Eq. (1) do not depend on the direction of the magnetization, and vary only when its magnitude is changed. Here $\lambda_1^{\alpha,0}$ determines the deformation in the basal plane of the crystal, and $\lambda_2^{\alpha,0}$ the deformation along the hexagonal axis. The remaining terms characterize the anisotropic magnetostriction, which involves the change in the orientation of the magnetization. The constants $\lambda_1^{\alpha,2}$ and $\lambda_2^{\alpha,2}$ describe the change in the volume and the change in the ratio c/a of the lattice parameters in the hexagonal structure while

preserving the hexagonal symmetry; $\lambda_3^{\alpha,2}$ represents the distortion of circular symmetry of the basal plane upon rotation of the magnetization vector in this plane; and $\lambda_4^{\alpha,2}$ characterizes the distortion of the right angle between the direction of the hexagonal axis and the basal plane.

The magnetostriction of cubic crystals is given by the formula

$$\lambda = \lambda_0 + \lambda_1^{\gamma,2} \left(\alpha_x^2 \beta_x^2 + \alpha_y^2 \beta_y^2 + \alpha_z^2 \beta_z^2 - \frac{1}{3} \right) + 2\lambda_2^{\gamma,2} (\alpha_x \alpha_y \beta_x \beta_y + \alpha_y \alpha_z \beta_y \beta_z + \alpha_x \alpha_z \beta_x \beta_z). \quad (2)$$

Here λ_0 is the isotropic magnetostriction, which does not depend on the direction of magnetization, while $\lambda_1^{\gamma,2}$ and $\lambda_2^{\gamma,2}$ are the anisotropic magnetostriction ($\lambda_1^{\gamma,2}$ characterizes tetragonal distortions, and $\lambda_2^{\gamma,2}$ rhombohedral distortions of the cubic structure). Instead of $\lambda_1^{\gamma,2}$ and $\lambda_2^{\gamma,2}$ one often uses the magnetostrictive constants λ_{100} and λ_{111} ; they are related by the equations: $\lambda_1^{\gamma,2} = (3/2)\lambda_{100}$, $\lambda_2^{\gamma,2} = (3/2)\lambda_{111}$.

One can describe the magnetostriction of a polycrystal by averaging Eqs. (1) and (2) over the different crystallographic directions. For example, for the longitudinal magnetostriction of an elastically isotropic polycrystalline cubic ferromagnetic we have^{13,14}

$$\lambda = \frac{1}{3} (2\lambda_{100} + 3\lambda_{111}). \quad (3)$$

3. RARE-EARTH AND ACTINIDE MAGNETICS WITH GIANT MAGNETOSTRICTION

a) Rare-earth metals and alloys

Table I presents the results of measuring the magnetostriction in polycrystalline specimens of the heavy rare-earth metals and the values of the magnetostriction of nickel, iron, and cobalt. We see that the magnetostriction of the rare-earth metals exceeds that of iron and nickel by factors of 30–50.

The magnetostriction of single crystals of rare-earth has been studied in Refs. 15–27. Table II gives the values of the magnetostrictive constants of rare-earth metal single crystals. We see that the anisotropic magnetostriction of rare-earth metals is very large. Especially large values ($\sim 10^{-2}$) are attained by the magnetostriction ($\lambda_2^{\alpha,2}$) of Tb, Dy, and Er along the hexagonal axis. It exceeds the longitudinal magnetostriction of iron and nickel crystals several hundredfold. The

TABLE I. Longitudinal magnetostriction of polycrystalline specimens of certain rare-earth metals and *d*-metals.

Metal	$\lambda_0 \cdot 10^6$	Temperature of measurements, K	References
Tb	1230	78	18
Dy	1400	78	9, 10
Fe	-10	300	14
Co	-71.4	300	14
Ni	-35	300	14

TABLE II. Magnetostrictive constants of heavy rare-earth metals at 4.2 K.

Magnetostrictive constants	Gd	Tb	Dy	Ho	Er
$\lambda_1^{\alpha, 0} \cdot 10^3$	-0.43 ²⁶	-4.27 ²⁷	-6.1 ²³		
$\lambda_2^{\alpha, 0} \cdot 10^3$	7.61 ²⁶	13.4 ²⁷	11 ²³		
$\lambda_1^{\alpha, 2} \cdot 10^3$	0.162 ²⁶	-11.6 ²³	12.9 ²⁴		
$\lambda_2^{\alpha, 2} \cdot 10^3$	-0.09 ²⁶	21 ¹⁹ 23.6 ²⁵	-9.1 ²⁰ 22 ¹⁹		
$\lambda^{\gamma, 2} \cdot 10^3$			8.7 ²⁰	-2.3 ²¹	-3.4 ²⁰
$\lambda^{\epsilon, 2} \cdot 10^8$			5.7 ²⁰		

dependence of the magnetostriction of a single crystal of Tb on a magnetic field applied along different crystallographic directions is shown in Fig. 1. In a field applied in the basal plane, the magnetostriction reaches saturation relatively rapidly, whereas in a field applied along the hexagonal axis, the isotherms of $\lambda(H)$ show no saturation up to fields ~ 150 kOe. This involves the large value of the anisotropy field of Tb along the hexagonal axis (~ 500 kOe).¹⁹

In the paramagnetic state the rare-earth metals possess a magnetostriction that, in a field $H > 100$ kOe, exceeds the magnetostriction of such ferromagnetics as nickel and iron²⁸ (Table III).

Large magnetostrictive changes in the dimensions of rare-earth metals and their alloys arise not only under the action of a field, but also of the temperature. Spontaneous magnetostriction leads to anomalies of thermal expansion (invar effects), which arise both in the basal plane and along the hexagonal axis c below the temperature of magnetic ordering. In the heavy rare-earth metals and their alloys one observes a paramagnet-antiferromagnet magnetic transition at the point θ_2 and an antiferromagnet-ferromagnet transition at the point θ_1 . In the temperature range from θ_1 to θ_2 these alloys have

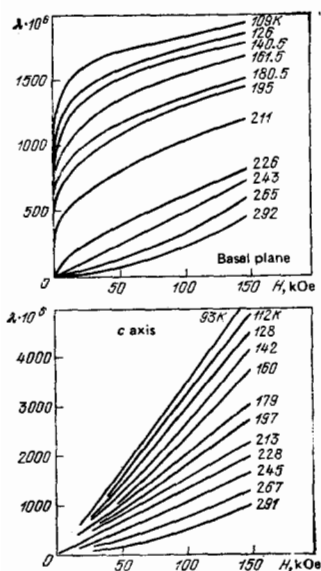


FIG. 1. Field-dependence of the longitudinal magnetostriction of a terbium single crystal.

TABLE III. Longitudinal magnetostriction of rare-earth metals in the paramagnetic region in a 144-kOe field at 300 K²⁸.

Metal	$\lambda_{ } \cdot 10^6$	Metal	$\lambda_{ } \cdot 10^6$
Tb	600	Ho	170
Dy	400	Er	-50

a helicoidal antiferromagnetic structure. At a value of the magnetic field exceeding a certain critical value H_{cr} , the helical antiferromagnetic structure breaks down.¹¹ Therefore such a field substantially alters the magnitude and character of the temperature-dependence of the thermal expansion. This effect is illustrated in Fig. 2, which shows²⁹ the curves for the temperature-dependence of the thermal expansion of crystals of Tb-Y alloys along the axis of easy magnetization (here this is the b axis in the basal plane) in a magnetic field $H = 55$ kOe, which exceeds H_{cr} and is directed along the b axis, and in zero field. The dotted lines in Fig. 2 are the phonon contributions to the thermal expansion. We see that curve 1 for the alloy Tb_{0.10}Y_{0.90} is mainly governed by the phonon contribution, since this alloy does not show magnetic ordering. For the rest of the alloys, owing to the imposition of a large spontaneous magnetostriction, the thermal expansion below the temperature of magnetic ordering has sharp anomalies in the temperature-dependence. The thermal expansion changes sharply when $H > H_{cr}$, often with sign change. Thus, one can "control" the thermal expansion here by using a magnetic field, i.e., by using the invar properties of the alloys.

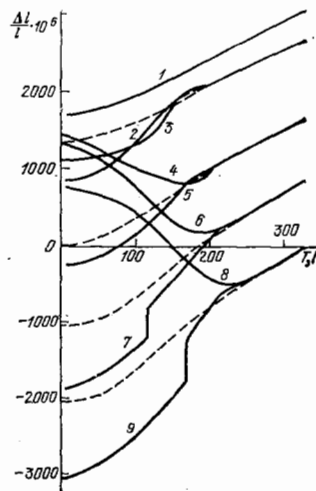


FIG. 2. Thermal expansion of single crystals of Tb-Y alloys along the b axis. The field $H = 55$ kOe lies along the b axis; the dotted lines are the phonon contributions to the thermal expansion.

Tb_{0.10}Y_{0.90}: 1 - $H > H_{cr, max}$ and $H = 0$;
 Tb_{0.50}Y_{0.50}: 2 - $H > H_{cr, max}$; 3 - $H = 0$;
 Tb_{0.49}Y_{0.51}: 4 - $H > H_{cr, max}$; 5 - $H = 0$;
 Tb_{0.885}Y_{0.115}: 6 - $H > H_{cr, max}$; 7 - $H = 0$;
 Tb_{0.81}Y_{0.19}: 8 - $H > H_{cr, max}$; 9 - $H = 0$.

TABLE IV. Magnetostriction of RFe₂-type intermetallic compounds.

Compound	4.2 K		300 K			References
	$\lambda_{111} \cdot 10^6$	$\lambda_{100} \cdot 10^6$	$\lambda_{111} \cdot 10^6$	$\lambda_{100} \cdot 10^6$	$\lambda_s^* \cdot 10^6$	
SmFe ₂	—	—	-2300	—	-1560	36, 37
TbFe ₂	4400	—	2500	—	1753	36, 37
DyFe ₂	—	-160	—	0	433	36, 37
HoFe ₂	776	-745	200	-67	85	10, 37
ErFe ₂	-1850	—	-280	—	-229	36, 37
TmFe ₂	-3620	—	-210	—	-123	41, 37

*) $\lambda_s = (2/3)(\lambda_{111} - \lambda_{100})$ at 25 kOe.

The effect of magnetic ordering on the crystal structure and lattice parameters of rare-earth metals has been studied by the x-ray method by Finkel' and his associates.³⁰

b) Intermetallic compounds of the rare earths

It has been shown³¹ that the intermetallic compounds of the type RFe₂ with a cubic crystal structure show giant magnetostriction, both at low temperatures and at room temperature. Table IV gives the values of the magnetostrictive constants of mono- and polycrystalline specimens of these compounds. The magnetostriction of TbFe₂ is especially large; here the dominant contribution to the magnetostriction of the polycrystal comes from the constant λ_{111} ; the constant λ_{100} is almost two orders of magnitude smaller.

Large magnetostriction is also observed in other compounds of the type RM₂, where M = Co, Mn, Al, Ni (Table V).

The spontaneous magnetostriction of these compounds causes distortions of the cubic structure to arise below the temperature of magnetic ordering. This is quite visible in Fig. 3, which shows the temperature-dependences of the crystal-structure parameters of the compounds TbCo₂ and DyCo₂. For TbCo₂ the axis of easy magnetization is the (111) direction. In this case the distortions are rhombohedral: below the Curie temperature the angle between two adjacent cube edges α differs from $\pi/2$. The formula (2) for the magnetostriction of a cubic crystal implies that: $\lambda_{111} = \epsilon = (\pi/2) - \alpha$ (in radians).

For DyCo₂ the axis of easy magnetization is parallel to (100). In this case tetragonal distortions arise,

TABLE V. Magnetostriction of RM₂-type intermetallic compounds at 4.2 K.

Compound	$\lambda_{111} \cdot 10^6$	$\lambda_{100} \cdot 10^6$	References	Compound	$\lambda_{111} \cdot 10^6$	$\lambda_{100} \cdot 10^6$	References
NdAl ₂	—	-1000	32	HoNi ₂	—	-1000	34
GdAl ₂	—	*)	32	ErNi ₂	—	*)	34
TbAl ₂	3000	—	32	TbCo ₂	4500	—	35
DyAl ₂	—	-2500	32	DyCo ₂	—	-2000	35
TbMn ₂	2800	—	33	HoCo ₂	260	-2200	35
TbNi ₂	1600	—	34	ErCo ₂	-2500	—	35
DyNi ₂	—	-1300	34				

*Value of the magnetostriction is less than 10⁻⁴.

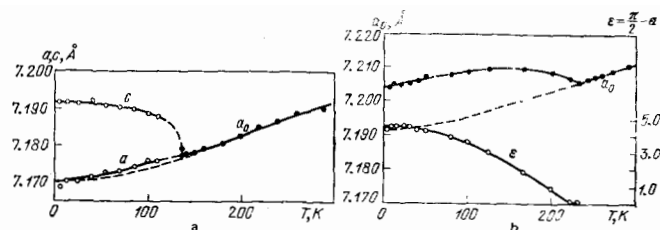


FIG. 3. Temperature-dependence of the crystal-structure parameters of the intermetallic compounds DyCo₂ (a) and TbCo₂ (b). The dots and the solid lines are the experimental data; the dotted lines are the phonon contribution to the lattice parameter.

which involve the magnetostrictive constant λ_{100} , with $\lambda_{100} = (2/3)[(c/a) - 1]$.

c) Garnet ferrites

The discovery of giant magnetostriction in the metals of the rare-earth group allowed one to assume the existence of analogous effects in the oxides and other dielectric compounds containing rare-earth ions. This hypothesis was first confirmed experimentally upon studying the magnetostriction of polycrystalline garnet ferrites (R₃Fe₅O₁₂, where R is a rare-earth ion) in the region of liquid-helium temperatures.⁴² Subsequently giant magnetostrictive effects have been observed in monocrystalline specimens of these garnets⁴³⁻⁴⁷ and in substituted compositions of the rare-earth garnet ferrites.⁴⁸ Table VI shows the results of measuring the magnetostriction in a set of garnet ferrite single crystals. Attention is called to the magnetostrictive deformation of the Tb₃Fe₅O₁₂ crystal. The value of λ_{111} in this compound is positive and considerably exceeds 10⁻³ at 4.2 K. The magnetostriction of this garnet owes its gigantic value to the rare-earth ion Tb³⁺. Therefore, even vanishingly small admixtures of terbium to yttrium iron garnet, whose magnetostriction is negative and amounts to ~10⁻⁶ (see Table VI), alter not only the magnitude, but also the sign of λ in this ferrite. This effect has been observed experimentally.⁴⁹

One of the features of the magnetic properties of the rare-earth ferrite garnets is that their magnetization increases considerably at temperatures below 100 K. Therefore, the largest values of magnetostrictive deformation in R₃Fe₅O₁₂ compounds are attained at the

TABLE VI. Magnetostriction of single crystals of ferrite garnets.

Garnet	$\lambda_{100} \cdot 10^6$		$\lambda_{111} \cdot 10^6$		References
	4.2 K	78 K	4.2 K	78 K	
Y ₃ Fe ₅ O ₁₂	-1.4	-1.0	-5.25	-3.6	46, 47
Sm ₃ Fe ₅ O ₁₂	—	+150	—	-483	48
Eu ₃ Fe ₅ O ₁₂	—	+86	—	+9.7	46
Gd ₃ Fe ₅ O ₁₂	+5.1	+4.0	-18.3	-5.1	43, 48
	+7.4	+4.4	-4.1	-4.7	45
Ho ₃ Fe ₅ O ₁₂	-665	-32.2	-632	-56.3	43, 46
Tb ₃ Fe ₅ O ₁₂	+1270	+7	+2460	+560	43, 46
Dy ₃ Fe ₅ O ₁₂	-1400	-254	-550	-145	44, 46
Er ₃ Fe ₅ O ₁₂	—	+10.7	—	-19.4	46
Tm ₃ Fe ₅ O ₁₂	—	+25	—	-31.2	46

*Extrapolation to 0 K.

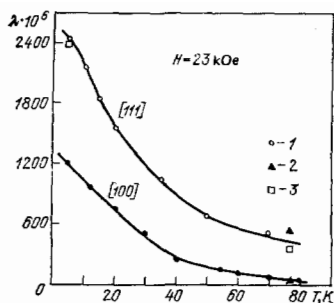


FIG. 4. Temperature-dependence of the magnetostriction of a single crystal of terbium iron garnet $Tb_3Fe_5O_{12}$ along the directions $\langle 111 \rangle$ and $\langle 100 \rangle$ according to the data of Refs. 43 (1), 46 (2), and 50 (3).

temperature of liquid helium. Figure 4 shows as an example the temperature-dependence of the constants λ_{100} and λ_{111} of $Tb_3Fe_5O_{12}$ as measured by different methods.^{43,46,50} We see that λ_{111} increases sharply with decreasing temperature, to reach the value 2420×10^{-6} at 4.2 K.

d) Compounds of the actinides

It has been established⁵¹⁻⁵⁸ that a number of ferromagnetic compounds of uranium having cubic and hexagonal structures possess very large magnetostrictions (Table VII). Magnetostriction in the uranium compounds can be measured without difficulty by x-ray diffraction. It is determined from the rhombohedral (or tetragonal) distortions of the hexagonal lattice. Figure 5 shows the data of measurements of the magnetostrictive constant λ_{111} of the compound U_3P_4 . The values obtained from measurements of the magnetostrictive deformations in a field coincide within the limits of error with the results of the x-ray measurements.

Table VIII presents the results of x-ray measurements of the anisotropic magnetostriction of the intermetallics of neptunium and plutonium.⁵⁹⁻⁶¹ We see that the magnetostriction in the actinide compounds reaches enormous values, in some cases even larger than in the rare-earth magnetics.

Interestingly, as x-ray studies have shown, magnetoelastic deformations of the structure are observed in actinide antiferromagnetic compounds only in cases in which the number of ferromagnetic interactions of the ion with its nearest neighbors exceeds the number of antiferromagnetic interactions. For example, if the antiferromagnetic ordering follows the type $+++--$,

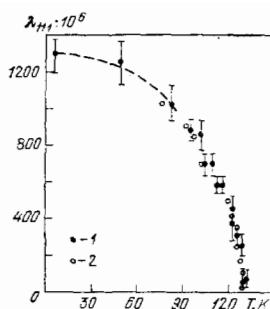


FIG. 5. Temperature-dependence of the magnetostrictive constant λ_{111} of the compound U_3P_4 . 1—data from x-ray measurements; 2—data from measurements of magnetostriction in a field.

one observes considerable magnetoelastic distortions of the crystal structure, while if the antiferromagnetic structure has the form $+-+ -$, the magnetostriction is small. The reason for this hasn't been finally clarified at present. Perhaps this phenomenon involves the fact that the structures in many actinide antiferromagnetics are noncollinear (the so-called multi- k structures⁶²).

e) Paramagnetic compounds of the rare earths

In the metals and compounds of the transition d-elements existing in the paramagnetic state, the magnetostriction generally does not exceed the value of 10^{-6} even in magnetic fields up to 100 kOe.⁶³ We should expect even smaller values of λ in the diamagnetic metals and alloys. However, there are exceptions: e.g., the longitudinal magnetostriction of a single crystal of Bi in a direction perpendicular to the trigonal axis at 78 K, according to the measurements of P. L. Kapitza, reaches 30×10^{-6} in a magnetic field of 250 kOe.⁶⁴

Yet the compounds of the rare-earth elements in the paramagnetic state also show magnetostrictive deformations comparable in magnitude with the magnetostriction of the magnetically ordered materials. Thus,⁵ it has been established in measuring the magnetostriction of the paramagnetic gallates⁶ $R_3Ga_5O_{12}$ and germanates⁶⁶ $Sr_3R_2Ge_3O_{12}$ with the garnet structure that, at temperatures below 20 K, the magnetostriction in a field ~ 30 kOe reaches values above 10^{-4} (Fig. 6). In the stated compounds the rare-earth ions occupy one type of structural sites of the garnet-dodecahedral or octahedral, and antiferromagnetic ordering arises in them only below a temperature ~ 0.5 K.⁶⁷ Just as in the ferrite garnets, the magnetostriction of the gallates and

TABLE VII. Magnetostriction of uranium compounds at 4.2 K.

Compound	Crystal structure	Temperature of magnetic ordering, K	$\lambda_{111} \cdot 10^6$	References	Compound	Crystal structure	Temperature of magnetic ordering, K	$\lambda_{111} \cdot 10^6$	References
U_3P_4	Tb_3P_4	138	1330	51, 53	UN	NaCl	87	-3470	57, 58
U_3As_4	To ditto	198	1140	52	UFe ₂	MgCu ₂	171	3000	53
US	NaCl	178	7000	57, 58	UGa ₂	AlB ₂ (hexag.)	125	4000*	55
USe	To ditto	160	5400	57, 58					

* λ_{111}^2 .

TABLE VIII. Magnetostriction of neptunium and plutonium compounds at 4.2 K.

Compound	Crystal structure	Temperature of magnetic ordering, K	Type of magnetic structure	$\lambda_{111} \cdot 10^6$	$\lambda_{100} \cdot 10^6$	References
PuP	NaCl	125	Ferro-	—	2070	61
NpC	ditto	300	Antiferro-	1540	—	59
			type 1 ($T > 220$ K)			
NpI'	»	130	Ferro- ($T < 220$ K)		—2800	59
			Antiferro-			
			type 1 ($T > 74$ K)			
			type + + + - - - ($T < 74$ K)			
NpAs	»	175	Antiferro-		—530 *	59
			type + + + - - - ($T > 140$ K)			
			type 1 ($T < 140$ K)			
NpFe ₂	MgCu ₂	~500	Ferro-	—8000		61
NpNi ₂	ditto	32	Ferro-	2860		61

*At 140 K.

germanates increases sharply with decreasing temperature, owing to the increase in the paramagnetic susceptibility.

At liquid-helium temperatures, magnetic fields of 30-kOe intensity give rise to giant (for paramagnetics) magnetostrictive deformations also in the tetragonal crystals LiRF_4 (scheelite structure), where $R = \text{Er, Tm, Ho, or Tb}$. According to the data of Ref. 68, the magnetostriction of a single crystal of LiErF_4 at 4.2 along the $\langle 100 \rangle$ axis in a field of 30 kOe reaches 3×10^{-4} . Here one observes a strong anisotropy of λ : when $H \parallel (110)$, the magnetostriction of the same crystal decreases by almost an order of magnitude.

The magnetostriction of the double fluorides of the rare earths gives rise to excitation in these paramagnetic crystals of a distinctive magnetoacoustic echo when acted on by an electromagnetic field pulse. This effect has been observed experimentally by S. A. Al'tshuler and his associates⁶⁹ in crystals of LiTbF_4 , LiHoF_4 , and LiErF_4 .

Recently giant magnetostriction has been found in the paramagnetic titanates of terbium $\text{Tb}_2\text{Ti}_2\text{O}_7$ and Tb_2TiO_5 .⁷⁰ The greatest value (5×10^{-4} in a 50-kOe

field) is reached at 4.2 K in the magnetostriction of the cubic compound $\text{Tb}_2\text{Ti}_2\text{O}_7$, having a pyrochlore-type structure.

4. A THEORETICAL MODEL OF GIANT MAGNETOSTRICTION

The relationship between the magnetostriction and the magnetization of a crystal is given by the well known thermodynamic relation

$$\left(\frac{\partial \lambda}{\partial H}\right)_{p_i} = \left(\frac{\partial I}{\partial p_i}\right)_H. \quad (4)$$

Here I is the magnetization, and p_i is the uniaxial stress acting in the direction of measurement of the magnetostriction. The magnetization I depends on the characteristics of the magnetic ions and their interactions among themselves and with the crystal field. The following sources of magnetostriction in a crystal are distinguished:

1. "Exchange" magnetostriction, caused by the variation in the exchange energy upon deformations; it can be isotropic or anisotropic, depending on the type of material.

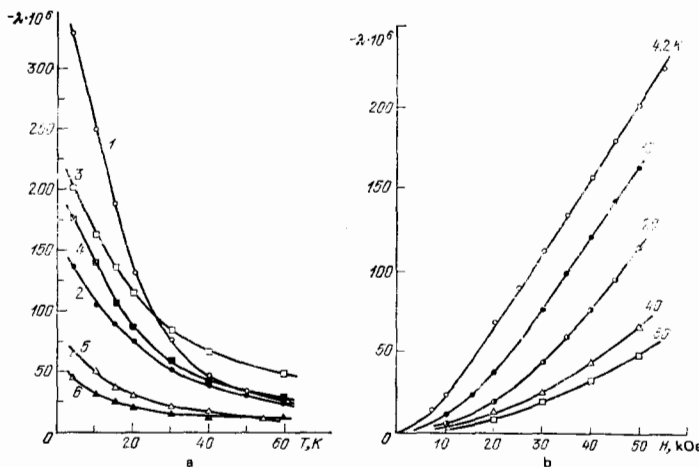


FIG. 6. Magnetostriction of rare-earth garnets, gallates, and germanates. (a) As a function of the temperatures in a field $H = 50$ kOe.⁶⁶ 1— $\text{Sr}_3\text{Ho}_2\text{Ge}_3\text{O}_{12}$, 2— $\text{Ho}_3\text{Ga}_5\text{O}_{12}$, 3— $\text{Ca}_3\text{Dy}_2\text{Ge}_3\text{O}_{12}$, 4— $\text{Dy}_3\text{Ga}_5\text{O}_{12}$, 5— $\text{Sr}_3\text{Er}_2\text{Ge}_3\text{O}_{12}$; 6— $\text{Er}_3\text{Ga}_5\text{O}_{12}$. (b) Isotherms for the paramagnetic garnet $\text{Ca}_3\text{Dy}_2\text{Ge}_3\text{O}_{12}$.

2. Magnetostriction caused by the orbital-crystal field and spin-orbital interactions; this magnetostriction is essentially anisotropic and arises in the regions of the magnetization curve where processes of rotation and displacement of domain boundaries occur.

3. Magnetostriction arising from the energy of the magnetic dipole interaction of the atoms; it is also anisotropic.

An essential point is that the rare-earth ions with unfilled 4f shells show a considerable value of the spin-orbital interaction. The splitting of the ground terms having a given L and S into multiplets amounts to a value of the order of 10^3 cm^{-1} . Yet the interaction of the rare-earth ions with the crystal field is smaller by one or two orders of magnitude, so that the ground state of a rare-earth ion is a state with a fixed principal quantum number J (J is a "good" quantum number). Consequently a feature of rare-earth magnetic materials is that the generation of magnetic properties in them is determined by the total mechanical angular momentum J which includes both the spin angular momentum S and the orbital angular momentum L . Thus, in contrast to the magnetic materials of the iron group, the orbital angular momentum in the rare earths is "not frozen".

The configuration of the electron cloud of 4f electrons responsible for the magnetism of rare-earth magnetic materials is not spherical, but sharply anisotropic, and is fixed by the total angular momentum $J = L + S$. If such an ion is "transferred" into a crystal lattice, the shape of the cloud is practically unaltered, since the spin-orbital interaction of the 4f electrons is far greater than the energy of the crystal field.

Rotation of the magnetic moment of a rare-earth ion in an external magnetic field reorients the electron cloud with respect to the crystalline environment. Since here the repulsion between the substantially asymmetric charge distribution of the given rare-earth ion and the surrounding ions will increase in one direction and decrease in another, the energy of the crystal will be minimized via deformation of the lattice. That is, anisotropic single-ion magnetostriction arises. In the case of a Gd^{3+} ion existing in the S state ($L=0$), the effect of magnetostrictive deformation is small, since the electron-density distribution of the 4f cloud is spherical here. This is confirmed by the experimental results for metallic gadolinium and its compounds.

What we have said above implies that the giant magnetostriction in the rare-earth ferro- and ferrimagnetics, and in the general case also in the paramagnetics, arises because the electron-density distribution of the 4f shell of the rare-earth ions behaves in the lattice like a "rigid", anisotropic electron cloud. Hence a rotation of the magnetic moment of the ion strongly deforms the crystal lattice.

The discussed model, which was initially developed for dielectric magnetic materials,⁷¹ can also be applied with a certain approximation for metallic rare-earth magnetic materials, in which the localized 4f electrons are screened from the action of the crystal field, by the conduction electrons as well as the $5s^2$ and $5p^6$

shells. Here an anisotropic magnetostriction can arise from two mechanisms:

- 1) orbital-crystal field interaction;
- 2) interaction of the cloud of conduction electrons with the crystal field.

However, the latter contribution to the giant magnetostriction of rare-earth metals is apparently small, since the magnetostriction of the oxide compounds of the rare earths, in which electric conductivity is practically absent, is just as large as in the rare-earth metals and their alloys (see Table VI).

The theoretical analysis conducted by Tsuya, Clark, and Bozorth⁷² gives the following expression for the change in the potential of the electrostatic field of a hexagonal crystal lattice upon deformation (in the point-charge approximation):

$$\delta V(r) = (\epsilon_{xx} + \epsilon_{yy})(2z^2 - x^2 - y^2)W_1^{2,2} + \epsilon_{zz}(2z^2 - x^2 - y^2)W_2^{2,2} + \left[\frac{1}{4}(\epsilon_{xx} + \epsilon_{yy})(x^2 - y^2) + \epsilon_{xy}xy \right]W^{3,2} + (\epsilon_{yz}yz + \epsilon_{zx}xz)W^{6,2}. \quad (5)$$

Here x , y , and z are the coordinates of the point at which the potential is being calculated, while the parameters of the interaction are:

$$\left. \begin{aligned} W_1^{2,2} &= \frac{qe}{2} R_0^{-3} P_2, \\ W_2^{2,2} &= -\frac{9qe}{7} R_0^{-3} P_4 + \frac{3qe}{14} R_0^{-3} P_2, \\ W^{3,2} &= -\frac{6qe}{7} R_0^{-3} P_2 + \frac{6qe}{7} R_0^{-3} P_4, \\ W^{6,2} &= \frac{3qe}{7} R_0^{-3} P_2 + \frac{24qe}{7} R_0^{-3} P_4. \end{aligned} \right\} \quad (6)$$

Here qe is the charge of the ion (with $q=3$ for trivalent rare-earth ions without allowance for screening), and P_2 and P_4 are lattice sums:

$$P_2 = R_0^3 \sum_n \frac{1}{2} (3z_n^2 - R_n^2) R_n^{-5}, \quad P_4 = R_0^3 \sum_n \frac{1}{8} (35z_n^4 - 30z_n^2 R_n^2 - 3R_n^4) R_n^{-7}. \quad (7)$$

As one can easily show, the latter depend on the parameters of the hexagonal close-packed lattice, and can be expressed in terms of the mean distance between adjacent atoms and of the deviation of this structure from an ideal hexagonal structure. Upon using the equivalent Stevens operators, we can transform in the expression for δV from the coordinates (x, y, z) to the components of the total angular momentum operator (J_x, J_y, J_z). Then we obtain the following expressions for the magnetoelastic interaction constants:

$$\left. \begin{aligned} B_1^{2,2} &\approx \alpha J \left(J - \frac{1}{2} \right) W_1^{2,2} \langle r_{4f}^2 \rangle, \\ B_2^{2,2} &\approx \alpha J \left(J - \frac{1}{2} \right) W_2^{2,2} \langle r_{4f}^2 \rangle, \\ B^{3,2} &\approx \alpha J \left(J - \frac{1}{2} \right) W^{3,2} \langle r_{4f}^2 \rangle, \\ B^{6,2} &\approx \alpha J \left(J - \frac{1}{2} \right) W^{6,2} \langle r_{4f}^2 \rangle. \end{aligned} \right\} \quad (8)$$

Here $\langle r_{4f}^2 \rangle$ is the mean square of the radius of the 4f electron shell. The quantities $W_k^{i,2}$ vary weakly on going from one rare-earth metal to another.

Thus, Ref. 72 implies that one can represent the magnetostrictive constants of the rare-earth metals at 0 K in the form

$$\lambda_k^{i,2} = D_k^{i,2} \alpha J \left(J - \frac{1}{2} \right) \langle r_{4f}^2 \rangle. \quad (9)$$

TABLE IX. Relative values of the theoretical magnetoelastic constant $\lambda^{\gamma,2}$ at 0 K for the heavy rare-earth metals.

Rare-earth metal	J	α	$\alpha J (J - \frac{1}{2})$	$(\frac{B}{B_{Dy}})^{\text{theor}} - (\frac{\lambda}{\lambda_{Dy}})^{\text{theor}}$	$\left\{ \frac{\lambda^{\gamma,2}(0)}{ \lambda^{\gamma,2}(0) _{Dy}} \right\}^{\text{exp}}$	$(B^{\gamma,2})_{\text{cm}^{-1}}^{\text{exp}}$
Tb	6	$-\frac{1}{99}$	$-\frac{1}{3}$	1.04	0.67	-235
Dy	15/2	$-\frac{2}{9.35}$	$-\frac{1}{3}$	1.00	1.00	-350
Ho	8	$-\frac{1}{15.3}$	$-\frac{2}{15}$	0.38	0.28	-97
Er	15/2	$\frac{4}{35.45}$	$\frac{2}{15}$	-0.37	-0.44	-154
Tm	6	$\frac{1}{99}$	$\frac{1}{3}$	-0.88	—	—
Yb	7/2	$\frac{2}{63}$	$\frac{1}{3}$	-0.84	—	—

The Stevens coefficient α characterizes the form of the 4f electron cloud. In the series of rare-earth elements β changes sign; in Tb, Dy, and Ho the coefficient α is negative (the 4f cloud is oblate), while in Er, Tm, and Yb it is positive, i.e., the 4f cloud is extended along the direction of the magnetic moment. Correspondingly the sign of $\lambda^{\gamma,2}$ changes in the series of rare-earth metals on going from Ho to Er.

The estimates made for the rare-earth metals of the magnetoelastic constants based on the theory of Ref. 72 exceed their experimental values by a factor of about 15. This involves the fact that the theory is rather crude, since, it takes no account, first, of the screening of the ion core by the conduction electrons, and second, of the band structure and features of the topology of the Fermi surface of the rare-earth metals, on which the redistribution of the conduction electrons around the ion core depends as the crystal is deformed. Nevertheless, as we see from Table IX, Eq. (9) qualitatively correctly predicts the sign change and the relative magnitudes of the magnetostrictive constants with increasing atomic number of the heavy rare earths.

A theory of single-ion magnetostriction has been developed by Slonczewski⁷³ for the cobalt ferrite spinels. The explanation presented above for giant magnetostriction is also based on a single-ion model. However, the latter takes into account the features of the electronic structure of the rare-earth ions, in particular the fact that the spin-orbital interaction is much larger in them than the interaction of the orbital angular momentum with the crystal field of the lattice (the "rigid" electron-cloud model). This enables one to explain the physical nature of the giant magnetostrictive deformations in rare-earth compounds possessing either dielectric or metallic properties.

The problem arises of how applicable the model of single-ion anisotropic giant magnetostriction is for actinide magnetic materials. The point is that the 5f electrons responsible for the magnetism of actinide magnetic materials are less localized than the 4f electrons in rare-earth magnetic materials. Hence these electrons in the compounds of the actinides can be delocalized and transfer to other ions, as indicated by the changes in the magnetic moments of actinide atoms in going from one compound to another. It has been found

that the degree of delocalization of the 5f electrons is determined by the distance between the actinide atoms. Undoubtedly this situation should lead to a difference in the magnetic properties of the two classes of magnetic materials. In particular, it should give rise to a difference in the mechanisms of the exchange interaction. On the other hand, the magnetic properties of actinide magnetic materials resemble in many ways those of the rare-earth magnetic materials. Above all, the similarity is manifested in the fact that both possess enormous values of the magnetic-anisotropy energy and of the magnetostriction. This is explained by the fact that, although the 5f shell lies closer to the periphery of the atom than the unfilled 4f shell in the rare earths, nevertheless the orbital angular momentum of the actinides exists in an "unfrozen" or "partially frozen" state, and their 5f electron cloud also has a nonspherical, anisotropic configuration, which gives rise in the actinide magnetic materials to giant anisotropic magnetostriction.

The development of a microscopic theory of magnetostriction would enable one to calculate the magnetostrictive constants from the microscopic parameters of the magnetic ions and the crystal and electronic structure. This faces considerable difficulties at present that involve the correct allowance for the changes in the crystal electrostatic field caused by deformation of the ion framework of the lattice and the redistribution of the conduction electrons upon deformation. Therefore a phenomenological method⁷⁴⁻⁷⁸ acquires great importance that is based on taking into account the different forms of interactions in a magnetic material and on employing the symmetry properties of the magnetic crystals.

At present the magnetostriction of rare-earth magnetic materials is analyzed in most experimental studies on the basis of the theory developed by E. Callen and H. Callen,^{77,78} in which the phenomenological approach is supplemented with a number of model constructs. In this theory one uses a Hamiltonian that includes the energy of isotropic and anisotropic exchange, the magnetic energy in the external field, and the Dzyaloshinskii interaction energy. The magnetoelastic interaction and the magnetic-anisotropy energy of the undeformed lattice are assumed small, whereby

one can treat them by using perturbation theory. The elastic energy is taken into account in the classical form. By using group theory while allowing for the symmetry requirements of the crystal, one can find the elastic component, as well as the magnetoelastic single-ion and two-ion components of the Hamiltonian.

By minimizing the free energy, one determines the equilibrium deformations and shows that the magnetostrictive deformation of a hexagonal crystal is described by Eq. (1).

The magnetostrictive constants are the products of the magnetoelastic constants and the spin correlation functions, which govern the temperature- and field-dependence of the magnetostriction:

$$\left. \begin{aligned} \lambda_1^{\alpha, 0} &= \sum_{f, g} \left[\frac{1}{3} D_1^{\alpha, 0}(f, g) - \frac{1}{2} D_2^{\alpha, 0}(f, g) \right] \mathcal{J}_{f, g}, \\ \lambda_2^{\alpha, 0} &= \sum_{f, g} [D_1^{\alpha, 0}(f, g) + D_2^{\alpha, 0}(f, g)] \mathcal{J}_{f, g}, \\ \lambda_1^{\alpha, 2} &= \sum_f \left[\frac{1}{3} B_1^{\alpha, 2} - \frac{1}{2} B_2^{\alpha, 2} \right] L_f \\ &\quad + \sum_{f, g} \left[\frac{1}{3} D_1^{\alpha, 2}(f, g) - \frac{1}{2} D_2^{\alpha, 2}(f, g) \right] L_{f, g}, \\ \lambda_2^{\alpha, 2} &= \sum_f \left[\frac{1}{3} B_1^{\alpha, 2} + B_2^{\alpha, 2} \right] L_f \\ &\quad + \sum_{f, g} \left[\frac{1}{3} D_1^{\alpha, 2}(f, g) + D_2^{\alpha, 2}(f, g) \right] L_{f, g}, \\ \lambda^{\gamma, 2} &= \sum_f B^{\gamma, 2} L_f + \sum_{f, g} D^{\gamma, 2}(f, g) L_{f, g}, \\ \lambda^{\epsilon, 2} &= \sum_f B^{\epsilon, 2} L_f + \sum_{f, g} D^{\epsilon, 2}(f, g) L_{f, g}. \end{aligned} \right\} \quad (10)$$

Here $B_i^{\alpha, l}(f)$ and $D_i^{\alpha, l}(f, g)$ are the constants for single-ion (interaction with the crystal field) and two-ion (exchange) magnetoelastic interactions, f and g are the indices of the sites, \hat{S}_f and \hat{S}_g are spin operators, and $\mathcal{J}_{f, g}(T, H)$ is the two-ion isotropic spin-correlation function:

$$\mathcal{J}_{f, g}(T, H) = \langle \hat{S}_f \hat{S}_g \rangle; \quad (11)$$

$L_{f, g}(T, H)$ is the two-ion longitudinal spin correlation function:

$$L_{f, g}(T, H) = \left\langle S_f^z \cdot S_g^z - \frac{1}{3} \hat{S}_f \hat{S}_g \right\rangle; \quad (12)$$

$L_f(T, H)$ is the one-ion longitudinal spin correlation function:

$$L_f(T, H) = \left\langle (S_f^z)^2 - \frac{1}{3} S(S+1) \right\rangle. \quad (13)$$

One can calculate the temperature- and field-dependences of the magnetostrictive constants by calculating the correlation functions on the basis of various physical models. For a broad class of theoretical methods (molecular field, random-phase approximation, Green's functions), the means of the single-ion correlation function are identical functions of the magnetization. The following relationship has been derived⁷⁸ for the single-ion magnetostrictive constant of order l :

$$\frac{\lambda_l(T, H)}{\lambda_l(0, 0)} = \hat{I}_{l+\frac{1}{2}} [L^{-1}(m)]. \quad (14)$$

Here $\hat{I}_{l+\frac{1}{2}}$ is the reduced hyperbolic Bessel function:

$$\hat{I}_{l+\frac{1}{2}}(x) = \frac{I_{l+\frac{1}{2}}(x)}{I_l(x)}, \quad (15)$$

while $L^{-1}(m)$ is the inverse Langevin function of the relative magnetization m :

$$m(T, H) = L(x) = \hat{I}_{\frac{3}{2}}(x) = \coth x - \frac{1}{x}. \quad (16)$$

In the paramagnetic region where $m \ll 1$, we have for $l = 2$:

$$\frac{\lambda(T, H)}{\lambda(0, 0)} = \frac{3}{5} m^2(T, H). \quad (17)$$

In the low-temperature region, the theory⁷⁸ for the harmonic magnetostrictive constants implies that

$$\frac{\lambda_l(T, H)}{\lambda(0, 0)} = m^{l(l+1)/2}. \quad (18)$$

This relationship had been established previously by Kittel and Van Vleck⁷⁹ and also by Turov and Mitsek.⁸⁰

In addition to the single-ion magnetocrystalline interaction, another possible mechanism responsible for giant magnetostrictive deformations is the two-ion exchange interaction. According to Eq. (10), the latter is included via the two-ion magnetoelastic interaction constants and the two-ion spin correlation functions in all the magnetostrictive constants. This interaction not only differs along different crystallographic axes, but in principle it can depend on the direction of the magnetization vector, similarly to the single-ion magnetic anisotropy.

The longitudinal spin two-ion correlation function $L_{f, g}$ varies as m^2 almost throughout the entire temperature range, apart from very low temperatures, where it is proportional to m^3 . As regards the isotropic correlation function $\mathcal{J}_{f, g}$, it is proportional to m^2 in the approximation of molecular-field theory. However, one must use more rigorous methods to calculate it near the Curie point. In particular, the theory of clusters and the random-phase approximation lead to substantial refinements in the temperature-dependence of magnetostriction.⁷⁸

5. STUDIES OF GIANT MAGNETOSTRICTION IN RARE-EARTH ALLOYS AND COMPOUNDS

The experimental data characterizing the values of the magnetoelastic contributions from the different interactions to the giant magnetostriction of rare-earth alloys and compounds are of great significance in developing a microscopic theory of magnetostriction.

One of the effective methods of determining the character of the magnetoelastic constants is to study the composition-dependence of the magnetostriction of alloys and mixed compounds of the rare-earth metals. If the magnetoelastic interaction is of single-ion type, then we can treat the magnetoelastic energy of the alloy as an additive sum of the magnetoelastic interactions of the individual atoms. In this case the magnetostrictive constants should depend linearly on the concentration of the components of the alloy. Yet if the magnetoelastic interaction is of exchange type, then it depends on the number of pairs of interacting atoms, and hence the magnetostrictive constants should vary quadratically upon changing the concentrations of the components.

Another way of elucidating the nature of magnetostriction consists in analyzing the temperature-dependences of the magnetostrictive constants.

In a single-ion model the temperature-dependence of the magnetostrictive constant $\lambda^{n,l}$ can be represented by Eq. (14), but in the low-temperature region (where the relative magnetization is $1 > m > 0.5$) by Eq. (18). For the second-order magnetostrictive constant ($l = 2$) we have $\lambda^{n,l} \sim m^3$.

At the same time, the exchange magnetostriction varies with the temperature in the same way as the exchange energy, which is proportional to the square of the magnetization over a broad temperature interval below the Curie point, i.e.,

$$\lambda_{\text{exch}}^{n,l} = \lambda_{\text{exch}}^{n,l}(0) m^2 \quad (19)$$

(deviations from this relationship for the exchange magnetostrictive constants can arise near 0 K^{74,77,78}).

Consequently the study of magnetostriction as a function of the concentration and the magnetization, while varying the temperature of the specimen, makes it possible to single out the contributions to the magnetostriction from the different interactions.

Let us examine in greater detail this method of singling out the different contributions to the magnetostriction of the heavy rare-earth metals on the example of the alloys Tb-Gd, Dy-Gd, Dy-Y, and Tb-Y.

The experimental study of the magnetostriction of these alloys^{22,33,81-85} has shown it to be characterized by a sharp anisotropy as a function of the directions of measurement and of the magnetic field. The magnetostriction is small in a magnetic field along the hexagonal c axis, which in these alloys is the axis of difficult magnetization, in the fields up to 40 kOe in which the measurements were performed. This is because, owing to the large uniaxial magnetic anisotropy in these alloys,⁸⁶ the magnetic moment deviates weakly from the b axis, which lies in the basal plane of the hexagonal crystal and is the axis of easy magnetization. If the magnetic field is applied in the basal plane, the magnetostriction along the hexagonal c axis also is small.

Giant magnetostriction in the ferromagnetic state is observed in the heavy rare-earth metals and their alloys in a field applied in the basal plane while it is measured along the a and b axes, which also lie in this plane. Let us examine the latter case in greater detail.

Figure 7 shows the temperature-dependence of the saturation magnetostriction $\lambda_s(b,c)$, $\lambda_s(b,b)$, and $\lambda_s(a,b)$ of a single crystal of the alloy Tb_{0.5}Gd_{0.5} (hereinafter the first index in the parentheses denotes the direction of the magnetic field, and the second index the direction of measurement). We see that, in the given alloy at 4.2 K, $\lambda_s(b,b)$ and $\lambda_s(a,b)$ have an absolute value greater than 1.5×10^{-3} , with $\lambda_s(b,b) > 0$ and $\lambda_s(a,b) < 0$. Thus, if the directions of the field and of measurement in the basal plane coincide, the sign of the magnetostriction is positive, while it is negative if they do not coincide.

We can describe this experimental fact by a relation-

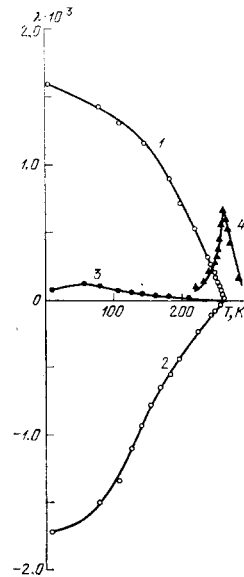


FIG. 7. Temperature-dependences of the saturation magnetostriction $\lambda_s(b,b)$ (1), i.e., with the direction of measurement along b and the field along b , $\lambda_s(a,b)$ (2), $\lambda_s(b,c)$ (3), and also the magnetostriction $\lambda_H(b,c)$ in a field $H = 14.5$ kOe (4) for a single crystal of the alloy Tb_{0.5}Gd_{0.5}.

ship that is a special case of Eq. (1). Actually, the field-induced magnetostriction along the b axis of a single-domain hexagonal crystal with $\mathbf{H} \parallel \mathbf{b} \parallel \mathbf{I}_s$ (H exceeds the saturation field) is

$$\lambda_s(b,b) = \lambda^{n,2} \sin^2 \varphi. \quad (20)$$

When $\mathbf{H} \parallel \mathbf{a} \parallel \mathbf{I}_s$, we have

$$\lambda_s(a,b) = -\lambda^{n,2} \cos^2 \varphi. \quad (21)$$

Here φ is the angle that the spontaneous-magnetization vector in the single-domain crystal forms with the axis of easy magnetization along the b axis.

Equation (15) implies that $\lambda_s(b,b) = 0$ in a single-domain crystal with the axis of easy magnetization along the b axis. The experimental observation that $\lambda_s(b,b) \neq 0$ (Fig. 7) involves the existence of a domain structure in the crystal.

In hexagonal crystals having a plane of easy magnetization there are three axes of easy magnetization and six directions of the vectors of the magnetic moments of domains. Therefore, for an identical volume of these domains, the field-induced magnetostriction along one of the b -type directions will be

$$\lambda(b,b) = \frac{1}{6} \sum_{i=1}^6 \lambda^{n,2} \sin^2 \varphi_i. \quad (22)$$

Here φ runs through the values $60^\circ n$. Hence we obtain $\lambda_s(b,b) = (1/2)\lambda^{n,2}$ as the saturation magnetostriction for crystals that have multi-domain structure at $H = 0$. Analogously we can find the saturation magnetostriction of a multidomain crystal along the b axis when the field is applied along the a axis: $\lambda_s(a,b) = -(1/2)\lambda^{n,2}$. Hence, when $\lambda^{n,2} > 0$, we have $\lambda_s(b,b) > 0$ and $\lambda_s(a,b) < 0$, which agrees with experiment (see Fig. 7).

Nonidentical absolute values of $\lambda_s(b, b)$ and $\lambda_s(a, b)$ are observed experimentally owing to the lack of a strict statistical distribution of the domains in real crystals over the six equally probable orientations of the magnetization. This can be caused by even slight defects and internal stresses in the crystals that arise in growing and processing them.

To answer the question of the nature of the field-induced giant magnetostriction $\lambda(b, b)$ and $\lambda(a, b)$ in the basal plane, let us examine the concentration- and temperature-dependence of the magnetostrictive constant $\lambda^{\gamma,2}$. The latter does not depend here on the initial domain distribution, and involves the orthorhombic distortions in the basal plane:

$$\lambda^{\gamma,2} = \lambda_s(b, b) - \lambda_s(a, b). \quad (23)$$

The interpretation of the results in the alloys of the heavy rare-earth metals with gadolinium and yttrium is considerably facilitated by taking into account the fact that the magnetostriction of gadolinium is considerably smaller (by an order of magnitude) than in the other rare earths, while yttrium is a Pauli paramagnetic. Hence, we can neglect the contribution of the Gd and Y ions to the magnetostriction.

Figure 8 shows the composition-dependence of the magnetostrictive constants $\lambda^{\gamma,2}(0)$ in terbium-gadolinium and dysprosium-gadolinium alloys.^{22,34} We see that one observes a linear increase in the magnetostrictive constant $\lambda^{\gamma,2}(0)$ within the limits of error with increasing content of dysprosium or terbium in the alloy. As we have noted above, this indicates a single-ion type of magnetostriction. Thus the measurements imply that the magnetostriction of the alloys of gadolinium with the heavy rare earths is mainly single-ion, and stems from the interaction of the anisotropic charge cloud of the 4f electrons of dysprosium (or terbium) with the crystal field of the lattice.

Figure 9 shows the dependence of the magnetostrictive constants $\lambda^{\gamma,2}$ of dysprosium-gadolinium alloys on the reduced temperature T/θ_2 (θ_2 is the temperature of magnetic ordering of the alloy). The theoretical $\lambda^{\gamma,2}(T)$ relationships are drawn there also for a single-ion model of the magnetostriction according to Eq. (14).

We see that the experimental temperature-dependences of the magnetostriction of dysprosium-gadolinium

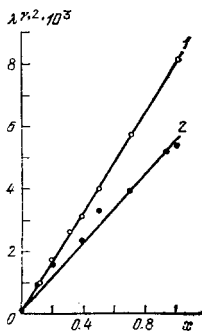


FIG. 8. Concentration-dependence of the constant $\lambda^{\gamma,2}$ characterizing the magnetostriction in the basal plane in the alloys $\text{Dy}_x\text{Gd}_{1-x}$ (1) and $\text{Tb}_x\text{Gd}_{1-x}$ (2).

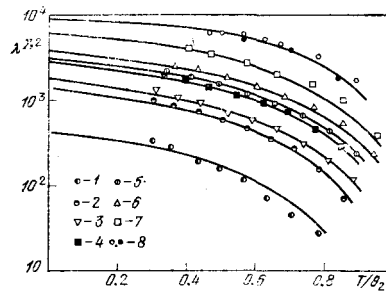


FIG. 9. Temperature-dependences of the magnetostrictive constants $\lambda^{\gamma,2}$ of $\text{Dy}_x\text{Gd}_{1-x}$ alloys. The symbols are the experimental data: 1— $x=0.046$; 2— $x=0.103$; 3— $x=0.183$; 4— $x=0.296$; 5— $x=0.378$; 6— $x=0.49$; 7— $x=0.7$; 8— $x=1.0$. The solid lines are the theoretical dependences for the model of single-ion magnetostriction.

alloys are described satisfactorily by the theoretical dependence for the model of single-ion anisotropy.

Figure 10 shows for the alloys $\text{Tb}_x\text{Y}_{1-x}$ and $\text{Tb}_x\text{Gd}_{1-x}$ the relationship of the normalized magnetostrictive constant $\lambda^{\gamma,2}$ to the relative magnetization of the terbium sublattice m_{Tb} .²³ In the alloys $\text{Tb}_x\text{Gd}_{1-x}$, m_{Tb} was found by solving the molecular-field equations for the magnetization.³⁶

The solid line (curve 2) in Fig. 10 has been constructed according to the formula (14) for single-ion magnetostriction. The dotted curve in Fig. 10 corresponds to the relationship for the exchange mechanism [Eq. (19)].

We see from Fig. 10 that the dependence of $\lambda^{\gamma,2}$ on the magnetization in the given alloys is close to that expected for single-ion contributions [Eq. (15)]. This allows us to conclude that the magnetostriction in the basal plane arises from the interaction of the orbital angular momentum of the 4f subshell of the rare-earth ion with the crystal field of the lattice.

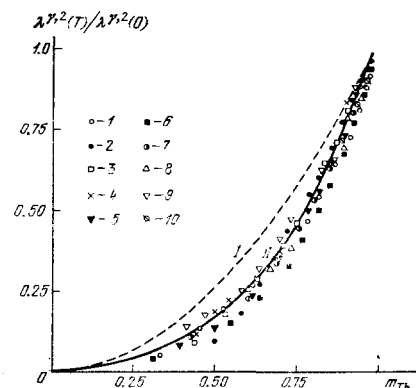


FIG. 10. Dependence of the relative value of the magnetostrictive constant $\lambda^{\gamma,2}(T)/\lambda^{\gamma,2}(0)$ on the relative magnetization m_{Tb} for $\text{Tb}_x\text{Gd}_{1-x}$ alloys for different values of x (1— $x=0.09$; 2—0.20; 3—0.39; 4—0.50; 5—0.70; 6—0.94) and for $\text{Tb}_x\text{Y}_{1-x}$ alloys (7— $x=1$; 8—0.91; 9—0.835; 10—0.50). Curve I has been obtained by Eq. (19), and II by Eq. (14).

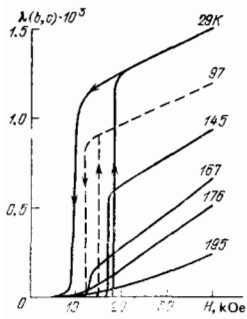


FIG. 11. Isotherms of the magnetostriction $\lambda(b, c)$ of a single crystal of the alloy $\text{Tb}_{0.63}\text{Y}_{0.37}$.

In the antiferromagnetic alloys Tb-Y and Dy-Y one observes, in addition to the magnetostriction in the basal plane, a different type of giant magnetostriction, namely along the hexagonal axis, which accompanies the breakdown of the antiferromagnetic helicoidal structure in these alloys in magnetic fields $H > H_{cr}$. When $H < H_{cr}$ it is small, but when $H > H_{cr}$ it increases sharply and reaches values $\sim 10^{-3}$ in the low-temperature region. This is implied by Fig. 11, which shows the isotherms of the magnetostriction $\lambda(b, c)$ in a field $H \parallel b$ along the c axis for a single crystal of the alloy $\text{Tb}_{0.63}\text{Y}_{0.37}$. According to the neutron-diffraction⁸⁷ and magnetic⁸⁸ studies, a helicoidal magnetic structure exists in this alloy below the antiferromagnetism-paramagnetism transition point θ_2 .

We shall call the jump in the magnetostriction along the c axis at $H = H_{cr}$ the "helicoidal" magnetostriction and denote it as λ_{sc} . It turns out that λ_{sc} in the alloys Tb-Y and Dy-Y is proportional to the square of the magnetization at $H = H_{cr}$ over a broad temperature range [Eq. (19)]. This is illustrated for the alloy $\text{Tb}_{0.63}\text{Y}_{0.37}$ by Fig. 12, which also calls attention to the slower decline of λ_{sc} with increasing temperature than that of $\lambda^{\gamma, 2}$.

As we have noted above, a proportionality of the magnetostrictive constants to the square of the magnetiza-

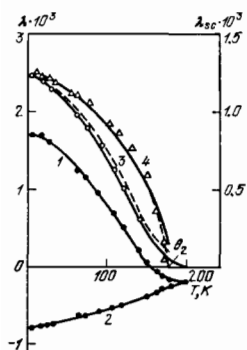


FIG. 12. Temperature-dependences of the saturation magnetostriction of the alloy $\text{Tb}_{0.63}\text{Y}_{0.37}$: $\lambda_s(b, b)$ (1) and $\lambda_s(a, b)$ (2), of the magnetostrictive constant $\lambda^{\gamma, 2}$ (3), and of the helicoidal magnetostriction λ_{sc} (4) for $H > H_{cr}$. The dotted curve is calculated by Eq. (15). A curve has been drawn through the experimental points that has been calculated by the formula $\lambda_{sc} = \lambda_{sc}^0 (I_s)^2$.

tion corresponds to an exchange mechanism, both in the ferromagnetic and in the helicoidal states. Therefore we can conclude that the "helicoidal" magnetostriction along the c axis arises from the change in the energy of the two-ion exchange interaction between the magnetic layers when the helicoidal magnetic structure breaks down. Moreover, a certain influence on its magnitude can be exerted by the change in the energy spectrum of the conduction electrons in the antiferromagnetism-ferromagnetism transition at $H > H_{cr}$.⁸⁹

Above we have examined the method of determining the magnetostrictive constant $\lambda^{\gamma, 2}$ from measurements of the magnetostriction induced by a magnetic field in the basal plane of the crystal. To determine the two-ion magnetostrictive constants $\lambda_1^{\alpha, 0}$ and $\lambda_2^{\alpha, 0}$, we require data on the spontaneous magnetostriction. One can find the spontaneous magnetostriction from the temperature-dependence of the thermal expansion below the temperature of magnetic ordering by subtracting the phonon contribution to the thermal expansion.⁸² Actually, in the low-temperature region ($1 > m > 0.5$), the theory of Callen and Callen⁷⁸ implies relationships that describe the dependence on the magnetization of the spontaneous magnetostriction along the crystallographic axes b , a , and c :

$$\begin{aligned} \frac{\Lambda_b}{m^2} &= \lambda_1^{\alpha, 0} + \lambda_6 m, \\ \frac{\Lambda_a}{m^2} &= \lambda_1^{\alpha, 0} + (\lambda_6 - \lambda^{\gamma, 2}) m, \\ \frac{\Lambda_c}{m^2} &= \lambda_2^{\alpha, 0} - \frac{1}{3} \lambda_2^{\alpha, 2} m. \end{aligned} \quad (24)$$

Here we have

$$\lambda_6 = -\frac{1}{3} \lambda_1^{\alpha, 2} + \frac{1}{3} \lambda^{\gamma, 2}. \quad (25)$$

Here we assume that the magnetization lies along the b axis, while the magnetostrictive constants $\lambda^{\gamma, 2}$, $\lambda_1^{\alpha, 2}$, and $\lambda_2^{\alpha, 2}$ are governed by the single-ion magnetocrystalline interaction.

Upon employing the magnetostrictive contributions to the thermal expansion, which coincide with the spontaneous magnetostriction when $m > 0.5$, together with the spontaneous magnetization $I_s(T)$ found from the magnetization curves, we can construct the dependence of Λ_b/m^2 and Λ_c/m^2 on the relative magnetization $m = I_s(T)/I_s(0)$ for the alloys terbium-yttrium, dysprosium-gadolinium, and terbium-gadolinium²³ (see Figs. 13 and 14). We see that these relationships are linear. That is, they are described by the formulas (24), which allows us to find the magnetostrictive constants $\lambda_1^{\alpha, 0}$, $\lambda_2^{\alpha, 0}$, λ_6 , $\lambda_2^{\alpha, 2}$, and knowing $\lambda^{\gamma, 2}$, to determine $\lambda_1^{\alpha, 2}$ from Eq. (25).

The values of the magnetostrictive constants $\lambda_1^{\alpha, 2}$ and $\lambda_2^{\alpha, 2}$ found for the rare-earth metals by other methods agree satisfactorily with those found by the method presented above (see Table II). Let us emphasize another important circumstance: an advantage of the given method is that it enables one to find the magnetostrictive constants $\lambda_1^{\alpha, 2}$ and $\lambda_2^{\alpha, 2}$ without applying strong fields comparable with the saturation fields of the rare-earth metals.

Analysis of the experimental data shows (see Table II) that the exchange contributions in Gd to the spontan-

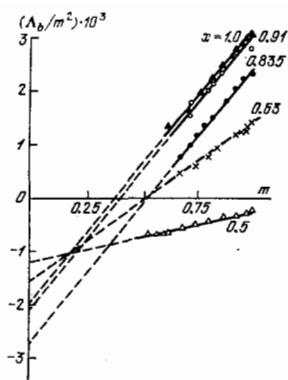


FIG. 13. Dependence of the spontaneous magnetostriction Λ_b , divided by the square of the relative saturation magnetization m on the value of m for $Tb_x Y_{1-x}$ for various values of x .

ous magnetostriction $\lambda_2^{\alpha,0}$ and $\lambda_1^{\alpha,0}$ exceed the single-ion contributions by an order of magnitude or more. We can explain this by the absence of orbital angular momentum ($L=0$) and the spherical character of the 4f electron subshell in the ground state of the Gd^{3+} ion.

In Tb, Dy, and Er and their alloys, the single-ion anisotropic magnetostrictive constants $\lambda_1^{\alpha,2}$, $\lambda_2^{\alpha,2}$, and $\lambda^{\gamma,2}$ are comparable in magnitude with the exchange magnetostrictive constants $\lambda_1^{\alpha,0}$ and $\lambda_2^{\alpha,0}$ (see Table II). This has the result that the single-ion magnetoelastic interaction, together with the exchange interaction, makes a considerable contribution to the thermal expansion of the rare-earth metals and their alloys.

Thus the experimental data given above show that the field-induced giant magnetostriction of the rare-earth metals is single-ion in type and arises from the interaction of the anisotropic electron shell of the 4f electrons with the crystal field.

One can also draw an analogous conclusion on the single-ion character of the anisotropic magnetostriction for the intermetallic compounds of the rare-earth metals with the 3d-transition metals. In particular, this is indicated by the linear dependence of the magnetostriction on the concentration that has been found in a set of quasibinary systems: $Gd_x Tb_{1-x} Fe_2$, $Ho_x Tb_{1-x} Fe_2$, $Pr_x Tb_{1-x} Fe_2$, etc.^{38 90-92}

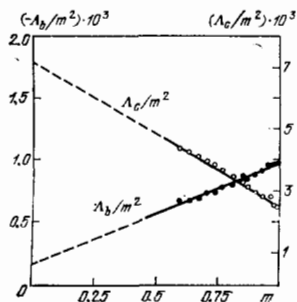


FIG. 14. Dependence of Λ_c/m^2 and Λ_b/m^2 on the relative saturation magnetization m for the alloy $Tb_{0.5} Gd_{0.5}$.

We note a feature of the RFe_2 compounds that is important for the practical aspect: giant magnetostrictive deformations are observed in them not only at low temperatures, but also at room temperature (see Table IV). This arises from the fact that a strong effective exchange field ($\sim 3 \times 10^6$ Oe) acts on the rare-earth ions in RFe_2 .^{93,94} This gives rise to a considerable magnetic moment of the rare-earth sublattice at room temperature and above, and hence, in line with Eq. (14), to giant magnetostriction.

It has been shown^{44-47,95} that the temperature-dependence of the magnetostriction of the ferrite garnets of the rare-earths and yttrium is well described within the framework of the single-ion theory, just as for the rare-earth metals. Here the magnetoelastic energy of the ferrite garnet amounts to the sum of the magnetoelastic interactions of each of the magnetic sublattices, while the temperature-dependence of the magnetostrictive constants is described by the relationships

$$\lambda^{\gamma,2} = \frac{3}{2} \lambda_{100} = -\frac{1}{c_{11}-c_{12}} \sum_n B^{\gamma,2}(n) \hat{I}_{\frac{5}{2}} \{L^{-1}[m_n(T)]\},$$

$$\lambda^{\epsilon,2} = \frac{3}{2} \lambda_{111} = -\frac{1}{2c_{44}} \sum_n B^{\epsilon,2}(n) \hat{I}_{\frac{5}{2}} \{L^{-1}[m_n(T)]\}.$$
(26)

Here the c_{iR} are the elastic constants, $B^{\gamma,2}(n)$ and $B^{\epsilon,2}(n)$ are the temperature-independent magnetoelastic interaction constants of the n th sublattice of the ferrite garnet, and the rest of the symbols are the same as in Eq. (14). Equations (26) imply that the temperature-dependence of the magnetostrictive constants is determined by the temperature variation of the magnetization of the corresponding sublattices. Here the contribution of the iron sublattice to the magnetostriction of the rare-earth ferrite garnets can be determined from measurements of the magnetostriction of yttrium iron garnet. Under the assumption that the temperature-dependences of the magnetizations of the iron sublattices in the rare-earth iron garnets are the same as for yttrium iron garnet, the values were determined in Ref. 43 of $B^{\gamma,2}$ and $B^{\epsilon,2}$ of the rare-earth sublattices of the iron garnets of terbium and holmium (per rare-earth ion):

$$Tb_3Fe_5O_{12}: \begin{matrix} B^{\gamma,2} = 160 \text{ cm}^{-1} \\ B^{\epsilon,2} = 3200 \text{ cm}^{-1} \end{matrix}, \quad Ho_3Fe_5O_{12}: \begin{matrix} B^{\gamma,2} = -360 \text{ cm}^{-1} \\ B^{\epsilon,2} = -170 \text{ cm}^{-1} \end{matrix}.$$

These coefficients exceed by a factor of more than 100 the corresponding magnetoelastic interaction constants of the iron sublattices in the iron garnets. They are comparable in order of magnitude with the magnetoelastic interaction constants of the rare-earth metals (see Table IX).

We should note that good agreement of the experimental temperature-dependences of the magnetostrictive constants of the rare-earth iron garnets with the theoretical formulas of (26) is observed only at temperatures above $T \approx 40$ K.^{43,44} This is illustrated by Figs. 15 and 16, which show the theoretical and experimental variations of the magnetostrictive constants of $Ho_3Fe_5O_{12}$ and $Dy_3Fe_5O_{12}$. There are several possible reasons for the deviation between experiment and the single-ion theory of magnetostriction in the region of liquid-helium temperatures. First, according to the

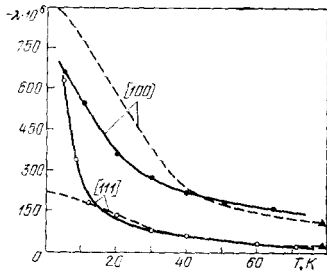


FIG. 15. Temperature-dependence of the magnetostriction of holmium iron garnet $\text{Ho}_3\text{Fe}_5\text{O}_{12}$. Dotted lines—theoretical data for $H=0$; solid lines—experimental data for $H=23$ kOe,⁴³ ▲—experimental data of Ref. 46.

existing neutron-diffraction data, noncollinear spin configurations arise in the iron garnets of holmium, terbium, etc., at low temperatures, whereas the theory⁹⁵ has been constructed for a Néel (collinear) cubic ferrimagnetic. Second, this theory assumes that the energy of the crystal field is much smaller than the exchange energy, which does not hold true for the iron garnets, especially at low temperatures. Moreover, the discrepancy of the formulas of (26) with experiment can arise from the inapplicability of the molecular-field theory near 0 K.

Studies have been performed^{45, 96-99} on the magnetostriction of single crystals of a series of iron-garnet systems in which the rare-earth was partially replaced by Y: $\text{Dy}_x\text{Y}_{3-x}\text{Fe}_5\text{O}_{12}$, $\text{Tb}_x\text{Y}_{3-x}\text{Fe}_5\text{O}_{12}$, $\text{Er}_x\text{Y}_{3-x}\text{Fe}_5\text{O}_{12}$, and $\text{Sm}_x\text{Y}_{3-x}\text{Fe}_5\text{O}_{12}$. Here it turned out that the magnetostrictive constants in most cases depend linearly on the concentration of the rare-earth ion (Fig. 17). This indicates that in these ferrimagnetics the magnetostriction arises either from the single-ion magnetoelastic interaction with the rare-earth sublattice, or from the magnetoelastic component of the rare-earth-iron exchange interaction, which also depends linearly on the concentration of the rare-earth ions. The problem of finding which of these mechanisms dominates requires further study. However, the results of Refs. 43-45, according to which the temperature-dependences of the magnetostriction of a set of rare-earth garnets in the temperature range 80-300 K is described by the formulas of (26), favor the single-ion mechanism.

At the same time, the concentration dependences of certain constants, in particular λ_{100} of terbium-yttrium

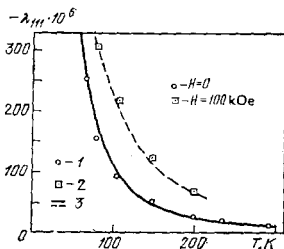


FIG. 16. Temperature-dependence of the magnetostriction of a single crystal of dysprosium iron garnet $\text{Dy}_3\text{Fe}_5\text{O}_{12}$ along the $\langle 111 \rangle$ axis.⁴⁵ 1—experimental data for $H=0$, 2—experimental data for $H=100$ kOe, 3—according to Eq. (26) of the single-ion theory.

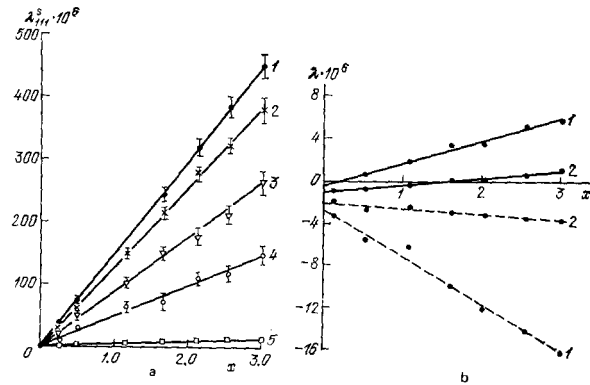


FIG. 17. Concentration-dependence of the magnetostriction constants of mixed ferrite garnets. a) λ_{111} — $\text{Tb}_x\text{Y}_{3-x}\text{Fe}_5\text{O}_{12}$: 1—78 K, 2—105 K, 3—125 K, 4—150 K; b) λ_{111} (dotted lines) and λ_{100} (solid lines) $\text{Er}_x\text{Y}_{3-x}\text{Fe}_5\text{O}_{12}$: 1—78 K, 2—293 K.

iron garnet and λ_{111} of samarium-yttrium iron garnet, are nonlinear. We can assume that in these cases the rare earth-rare earth magnetoelastic interaction, which depends quadratically on the concentration of the rare-earth ions, contributes to the magnetostrictive constants. Another possible reason for this nonlinearity is the change in the parameters of the crystal field upon replacing the rare earth with yttrium, which alters the single-ion magnetostriction. This change involves the differing dimensions of the atoms of these elements: upon substitution the configuration of the crystal environment of the rare-earth ions is changed. This effect is especially significant in the samarium-yttrium garnets, since in this system the crystal lattice parameter is altered more strongly than in the other garnets.

As is known,¹⁰⁰ in the rare-earth iron garnets the negative exchange interaction of the rare-earth and iron sublattices tends to orient the magnetic moments of the sublattices antiparallel to one another, while the interaction of the magnetic moments of the sublattices with the external field tends to make them parallel. Owing to the competition between these factors, in a certain range of fields the magnetic moments of the iron and rare-earth sublattices are oriented at an angle to one another and to the direction of the external field—a field-induced noncollinear structure arises. The formation of a noncollinear structure gives rise to anomalies in the field-dependences of the magnetostriction. This is quite visible in Fig. 18, which shows the field-dependence of the magnetostriction of holmium iron garnet¹⁰¹: when a certain field is reached that depends on the temperature, the magnetostriction passes through a minimum. Comparison with the data of other experiments shows that the field at the maximum corresponds to the field for transition to the noncollinear phase. The appearance of anomalies in the field-dependences of the magnetostriction upon transition to the noncollinear phase stems from the fact that a component of transverse magnetostriction arises that has a different sign from the longitudinal striction when the magnetic moment of the rare-earth sublattice deviates from the field direction.

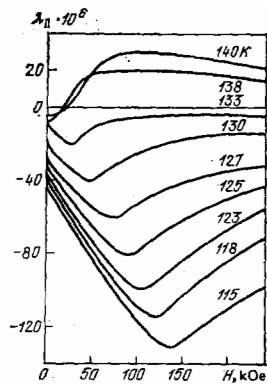


FIG. 18. Field-dependence of the longitudinal magnetostriction of holmium iron garnet $\text{He}_3\text{Fe}_5\text{O}_{12}$ near the magnetic-compensation temperature ($T_{\text{comp}} = 133 \text{ K}$).

As we have already noted, the interaction of the anisotropic electron cloud of rare-earth ions having $L \neq 0$ with the crystal field of the lattice gives rise to giant magnetostrictive deformations, even in crystals that exist in the paramagnetic state. Here the character and features of the magnetoelastic properties of the rare-earth gallates, germanates, fluorides, etc., are mainly determined by the symmetry of the intracrystalline fields and the structure of the energy levels of the rare-earth ion. Let us examine briefly as an example a single-ion mechanism that gives rise to giant magnetostriction in the paramagnetic crystals of the rare-earth fluorides.⁶⁸

The Hamiltonian of a rare-earth ion in a paramagnetic crystal can be represented in the form

$$\mathcal{H} = \mathcal{H}_0 + \mathcal{H}_z + \mathcal{H}_d.$$

Here \mathcal{H}_0 is the energy of the ion in the crystal field, $\mathcal{H}_z = g_J \mu_B H \cdot J$ is the Zeeman energy, and \mathcal{H}_d is the change in the energy of the ion in the crystal field caused by the lattice deformation. If the difference between the energies of the first excited Stark sublevel and the ground sublevel of the rare-earth ion obeys $\Delta \gg kT$ (in LiErF_4 the value of $\Delta = 18.2 \text{ cm}^{-2}$), then one can assume only the ground state to be filled in the crystal field, and treat \mathcal{H}_z as a perturbation along with \mathcal{H}_d . The energy \mathcal{H}_d can be written in terms of linear combinations of the displacements of the sublattices of the magnetically equivalent rare-earth ions and of the compounds of the deformation tensor, which transform according to the irreducible representations of the symmetry group of the given ion.

Upon using the condition of minimum free energy of the elastically deformed paramagnetic (in the absence of internal stresses), the authors of Ref. 68 expressed the components of the deformation tensor in terms of the electron-phonon interaction constants, which are calculated within the framework of the exchange-charge model, just like the crystal-field parameters. From the calculations they derived the following formula for the magnetostriction of the paramagnetic crystal:

$$\lambda = AH^2 + CH \tanh \frac{g\mu_B H}{2kT}. \quad (27)$$

Here A and C are functions of the direction cosines of the vectors H and of the direction of measurement. The satisfactory agreement of the theory with experiment for the LiErF_4 single crystal confirms the single-ion character of the magnetostriction in rare-earth paramagnetics.

One of the features of the magnetostriction of paramagnetic rare-earth compounds is that the action of an external magnetic field gives rise to two contributions to the magnetic moment of the crystal at low enough temperatures: an increase of the intrinsic (orientation-al) magnetic moment, which involves a change in the occupancy of the lower sublevels of the rare-earth ions in the crystal field, and a magnetic moment induced by the external magnetic field (Van Vleck paramagnetism). Under conditions of paramagnetic saturation of the ground state, the prevailing contribution to the resultant deformation of the crystal lattice in the external field comes from the magnetostriction caused by the induced moment. In this case, as measurements on LiErF_4 show,⁶⁸ the magnitude of the magnetostriction ceases to depend on the temperature, and varies in the external field proportionally to H^2 , both in weak and strong magnetic fields.

Since the intrinsic magnetic moment differs from zero only for ions having a degenerate ground state, one can distinguish the contributions mentioned above by studying the magnetostriction of Van Vleck paramagnetics, for which the ground state is a singlet. The measurements¹⁰² of the magnetostriction of a LiTmF_4 crystal have shown the existence at 4.2 K of a magnetostriction $\sim 10^{-3}$. According to the spectroscopic data in this paramagnetic the singlet Tm^{3+} in the crystal field of S_4 symmetry is separated from the nearest excited level by an energy gap $\Delta \approx 30 \text{ cm}^{-1}$. Hence a sufficiently strong magnetic field ($\mu_B H \approx \Delta$) gives rise to a magnetization $M \approx \mu_B H / \Delta$, which yields a giant magnetostrictive effect.

Now let us formulate the conditions for appearance of giant magnetostriction in a material. As the experimental data presented above imply, the first necessary condition for appearance of giant magnetostriction is a large concentration of ions of the rare earths or actinides having an "unfrozen" orbital angular momentum.

The magnitude of the magnetostriction also depends on the degree of orientation of the magnetic moments of the ions, i.e., the magnetization. As we know, the magnetization at a given temperature is determined by the Boltzmann factor $\exp[\mu_B g_J J(H + H_{\text{eff}})/kT]$, where H is the external magnetic field, and H_{eff} is the effective field of the exchange interaction acting on the rare-earth ion. The greatest magnetization, which corresponds to the maximum degree of orientation of the magnetic moments of the ions, arises under the condition

$$\mu_B g_J J (H + H_{\text{eff}}) \gg kT. \quad (28)$$

This condition determines the magnitude of the local magnetostrictive deformations of the crystal lattice arising from the interaction of the electron cloud with the crystal field, and hence, the temperature interval

in which one observes giant magnetostriction. As we have noted above, e.g., in the RFe_2 compounds, we have $H_{eff} \approx 3 \times 10^6$ Oe. Therefore giant striction is observed in these compounds even at temperatures above room temperature. This enhances considerably the potentialities of its practical application.

Thus, the second necessary condition for obtaining giant magnetostriction in a material is that the energy of interaction of the magnetic moments of the ions of the rare earth or actinide with the effective exchange and external magnetic fields must considerably exceed the energy of thermal motion.

As the measurements have shown,¹⁰³⁻¹⁰⁵ the alloys of the rare-earth metals with iron and cobalt, which have hexagonal and rhombohedral lattices with a single axis of easy magnetization (e.g., RCo_3 and R_2Co_{17} ; see also Ref. 106), possess a striction relatively small in magnitude, although their Curie points are high. Yet the exchange field H_{eff} acting on the rare-earth ions is of the same order of magnitude as in the compounds with a cubic lattice. This is explained by the fact that, in the presence of a strong spontaneous magnetostrictive deformation of the crystal lattice, the magnetostrictive effect induced by the external magnetic field proves to be relatively small if the material possesses a single axis of easy magnetization, while the field does not give rise to a substantial rotation of the spontaneous magnetization owing to the large magnetic anisotropy. In these magnetic materials processes mainly occur of shift of the 180° domain boundaries. However, these do not yield a magnetostrictive deformation, since striction is an "even" effect.

In magnetic materials having a cubic crystal lattice (RFe_2 , garnets, etc.), there are several axes of easy magnetization, while in the rare-earth metals there is a plane of easy magnetization (basal plane), in which three axes of easy magnetization lie. When an external magnetic field is applied, processes arise here of shift of domain boundaries that make a considerable contribution to the magnetostriction. Moreover, in the case of the rare-earth metals a large contribution comes from processes of rotation of the magnetic moment in the basal plane against the forces of magnetic anisotropy.

Hence the third necessary condition for obtaining giant magnetostriction in a material is the presence in the crystal lattice of several axes of easy magnetization. This condition is satisfied by a cubic structure and by a hexagonal lattice having a plane of easy magnetization.

$$\Delta K_1^{ME} = \frac{9}{2} \lambda_1^{\alpha,0} [(c_{11} + c_{12}) \lambda_1^{\alpha,2} - c_{13} \lambda_2^{\alpha,2}] + 3 \lambda_2^{\alpha,0} [c_{13} \lambda_1^{\alpha,2} - (2c_{13} + c_{33}) \lambda_2^{\alpha,2}]. \quad (30)$$

We note, as we see from (30), that this contribution is determined by the products of the magnetostrictive constants of exchange origin ($\lambda_1^{\alpha,0}$ and $\lambda_2^{\alpha,0}$) with the single-ion magnetostrictive constants ($\lambda_1^{\alpha,2}$ and $\lambda_2^{\alpha,2}$). This is a consequence of the general relationship for the magnetoelastic contribution to the anisotropy derived in Ref. 74, which implies that the magnetoelastic contri-

We note that a large magnetostriction can also be observed in the direction of difficult magnetization in uniaxial ferromagnetics in fields comparable with the effective field of the magnetic anisotropy. In antiferromagnetics, in which the magnetic moment of the ion is "bound" to the axis of antiferromagnetism, evidently, for analogous reasons the magnetostriction in a field must be small (an example of this may be the rare-earth orthoferrites).

6. THE EFFECT OF GIANT MAGNETOSTRICTION ON THE MAGNETIC ANISOTROPY AND THE ELASTIC PROPERTIES OF RARE-EARTH AND ACTINIDE MAGNETIC MATERIALS

Giant magnetostriction exerts a substantial effect, not only on the magnetic properties, but also on other properties of rare-earth and actinide magnetic materials. As we have already noted in Sec. 3, giant magnetostriction strongly alters the temperature-dependence of the crystal-structure parameters. In a number of cases this leads to the so-called invar effect—a thermal-expansion coefficient close to zero (see Fig. 2). In this section we shall treat in detail the effect of giant magnetostriction on the magnetic anisotropy and the elastic moduli.

As we know, the magnetic anisotropy is characterized by the energy that must be spent to turn the magnetic moments from the direction of easy magnetization to the direction of difficult magnetization. In this rotation (if the rotation processes occur at constant pressure), magnetostrictive deformations arise. Hence the magnetoelastic interaction energy is altered, and thus this interaction contributes to the energy of magnetic anisotropy.

As has been shown, e.g., by Kittel,¹³ for a cubic crystal the magnetoelastic contribution to the first constant of cubic magnetic anisotropy is

$$\Delta K_1^{ME} = \frac{9}{4} [(c_{11} - c_{12}) \lambda_{100}^2 - 2c_{44} \lambda_{111}^2] \quad (29)$$

(The c_{ij} are the elastic constants).

The magnetoelastic contribution to the uniaxial anisotropy constants of hexagonal crystals can be easily derived by employing the results of Refs. 107 and 108. The complete expressions are very unwieldy. Hence we shall present only an approximate formula for the magnetoelastic contribution to K_1 of a hexagonal crystal that has been derived without allowing for the magnetostrictive constants $\lambda^{1,2}$ and $\lambda^{e,2}$:

tribution to the anisotropy constant (n th order in the direction cosines) is proportional to the product of constants of orders n_1 and n_2 in the direction cosines, with $n_1 + n_2 = n$.

We can estimate by the formulas given above the order of magnitude of the magnetoelastic contribution to

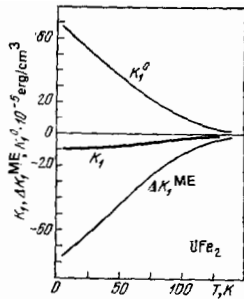


FIG. 19. Temperature-dependence of the measured first anisotropy constant K_1 , the magnetoelastic contribution ΔK_1^{ME} to this constant, and the anisotropy constant K_1^0 of the undeformed lattice of the compound UFe_2 .

the anisotropy energy of rare-earth and uranium compounds. If we assume that $\lambda^{n,l} \approx 10^{-3} - 10^{-2}$ and $c_{ij} \approx 10^{12}$ dynes/cm³, we find $\Delta K_1^{\text{ME}} \approx 10^6 - 10^8$ erg/cm³. As Eqs. (29) and (30) imply, the magnetoelastic contribution to the anisotropy will be large only when the magnetostriction is anisotropic, i.e., the different magnetostrictive constants have substantially different values. Yet if the magnetostriction is large but isotropic, the magnetoelastic contribution to the anisotropy constant will be small.

The effect of the magnetoelastic interaction on the magnetic anisotropy is quite visible in the example of the cubic compound UFe_2 .⁵⁶ This compound has a small magnetic anisotropy (Fig. 19), comparable in magnitude with that of pure iron and of the compound YFe_2 , which is isostructural with UFe_2 . At the same time, as we have noted above (see Table VII), the magnetostriction of UFe_2 is large ($\lambda_{111} = 3000 \times 10^{-6}$ at 4.2 K). Hence the energy of magnetoelastic interaction is also large. The results of the calculation for this compound of the magnetoelastic contribution to the first anisotropy constant of UFe_2 by Eq. (29), with allowance for the condition $\lambda_{111} \gg \lambda_{100}$, are also given in Fig. 19. We see that in absolute magnitude ΔK_1^{ME} exceeds manifold the measured anisotropy constant K_1 . The measured anisotropy constant equals the sum of the magnetoelastic contribution ΔK_1^{ME} and the anisotropy constant K_1^0 of the undeformed lattice:

$$K_1 = K_1^0 + \Delta K_1^{\text{ME}}. \quad (31)$$

Figure 19 shows the temperature dependence of the anisotropy constant K_1^0 of the undeformed lattice of the compound UFe_2 as determined from the experimental data by Eq. (31). We see from the diagram that $K_1^0 \gg K_1$. Thus the small value of the magnetic anisotropy of this compound arises from the "fortuitous" compensation of two large contributions: the anisotropy of the undeformed lattice and the anisotropy arising from the magnetoelastic interaction.

An analogous situation exists in the terbium-ytterbium iron garnets $\text{Tb}_x\text{Y}_{3-x}\text{Fe}_5\text{O}_{12}$.^{97,108} The experimental concentration-dependences of the first magnetic-anisotropy constant of these ferrimagnetics at the temperature 90 K are shown in Fig. 20, where the dependence of the magnetoelastic contribution to the anisotropy on

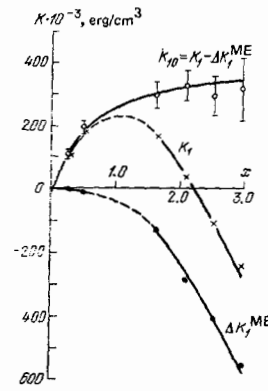


FIG. 20. Concentration-dependences of the first magnetic anisotropy constant K_1 , of the magnetoelastic contribution ΔK_1^{ME} to this constant, and of the anisotropy constant K_1^0 of the undeformed lattice of mixed ferrite garnets $\text{Tb}_x\text{Y}_{3-x}\text{Fe}_5\text{O}_{12}$ at 90 K.

the terbium content is also given for this temperature. We see that the magnetoelastic contribution to the first anisotropy constant prevails at a large terbium content: it is larger in absolute magnitude than the measured anisotropy constant. With decreasing terbium content, the magnetoelastic contribution declines more rapidly than the magnetic-anisotropy constant of the undeformed lattice. At a critical terbium content the magnitude of ΔK_1^{ME} becomes smaller than K_1^0 : at this concentration the measured anisotropy constant changes sign.

The magnetoelastic interaction influences just as substantially the magnetic anisotropy of the intermetallic compounds RFe_2 . It has been shown^{109,110} that one must take into account the magnetoelastic contribution to the first anisotropy constant to describe theoretically, in the model of single-ion anisotropy, the spin-reorientation phase diagrams in the mixed compounds $\text{Ho}_x\text{Tb}_{1-x}\text{Fe}_2$ and $\text{Dy}_x\text{Tb}_{1-x}\text{Fe}_2$. This is quite visible from comparing the experimental phase diagram of $\text{Dy}_x\text{Tb}_{1-x}\text{Fe}_2$ with the theoretical diagrams calculated with or without account taken of the magnetoelastic interaction (Fig. 21).

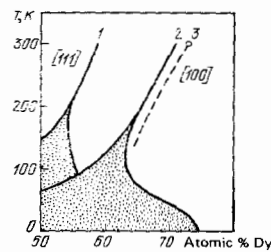


FIG. 21. Magnetic phase diagram of the mixed compounds $\text{Dy}_x\text{Tb}_{1-x}\text{Fe}_2$. 1—theoretical calculation according to the model of single-ion anisotropy without allowing for the magnetoelastic interaction; 2—theoretical calculation with allowance for the magnetoelastic interaction; 3—experimental data. The lines are shown that separate the phases in which the directions of easy magnetization are axes of the type $\langle 111 \rangle$, $\langle 100 \rangle$, or directions lying in planes of the type $\langle 110 \rangle$ (dotted).

Now let us examine the effect of giant magnetostriction on the elastic properties. Owing to the magnetoelastic interaction, application of external stresses to a ferromagnetic alters its magnetic state: a rearrangement of the magnitude and direction of the magnetization in the domains change. In turn, these changes give rise to additional changes in the dimensions of the specimen of material. This phenomenon is called mechanostriiction. The addition of the mechanostriictive deformation to the ordinary elastic deformation alters the elastic moduli of the magnetic material (the Young's modulus E and the shear modulus G for a polycrystal). This change depends both on the temperature and on the external magnetic field. Upon decreasing the temperature, when the paramagnetic state is superseded by the ferromagnetic state, anomalies arise in the temperature-dependence of the elastic moduli. In the region of the Curie point they are manifested as a jump or a break, e.g., in the $E(T)$ curve. Application of a magnetic field alters the magnitude of the mechanostriiction, and correspondingly, of the elastic moduli. This phenomenon is called the ΔE effect (for the Young's modulus). In strong fields in which the magnetic material is saturated, external stress ceases to affect the magnetic state, while the modulus attains the value E_s .

One usually takes the magnitude of the ΔE effect to be the field-dependent relative change in E as compared with the modulus E_0 of the material in the demagnetized state, i.e., $(E - E_0)/E_0$. In the simplest cases we can consider the magnitude of the total magnetic anomaly of the modulus $E_p - E_0$ (where E_p is the extrapolated modulus that the paramagnetic would have if it existed at the given temperature) as being equal to the maximal ΔE effect $E_s - E_0$. As energy considerations imply, this latter quantity is proportional to the energy of magnetoelastic interaction and inversely proportional to the energy opposing the change in the magnetic state under the action of elastic stresses (the magnetic-anisotropy energy, the energy of displacement of domain boundaries, etc.). Calculations show¹¹¹ that for various processes—rotation against the forces of cubic or uniaxial anisotropy, shift of domain boundaries, etc.—the magnitude of the maximal ΔE effect divided by E_s can be represented in the form

$$\Delta\left(\frac{1}{E}\right) = \frac{E_s - E_0}{E_s E_0} = A \frac{\lambda^2 \gamma_0}{I_s^2} \quad (32)$$

Here λ is the corresponding magnetostrictive constant, χ_0 is the initial susceptibility of the given magnetization process, I_s is the saturation magnetization, and A is a numerical constant of the order of unity (we note that $A = 0$ for processes of displacement of 180° domain boundaries).

In the rare-earth and actinide compounds, for which λ is large, we should expect large anomalies in the elastic properties, especially in cases in which the energy that stabilizes the magnetic state, e.g., the magnetic anisotropy, is small. Actually, even the first measurements in polycrystals of rare-earth metals^{15,112} showed large anomalies of the Young's and shear moduli in the magnetically ordered state. These

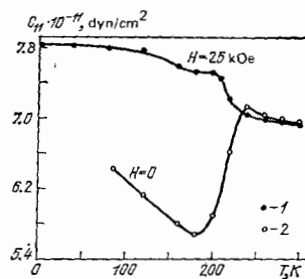


FIG. 22. Temperature-dependences of the elastic constant c_{11} of terbium in zero field (2) and in a 25-kOe field (1).

data have been subsequently confirmed by measurements of the elastic constants of single crystals of the rare-earth metals and their alloys.¹¹³⁻¹¹⁵ As an example, Fig. 22 shows the temperature-dependence of the elastic constant c_{11} of a single crystal of terbium. We see that c_{11} in zero field sharply declines below the temperature of magnetic ordering (230 K). Application of a field removes this anomaly.

In connection with possibilities of practical application (see Sec. 7), the magnetoelastic properties of RFe_2 -type compounds as well as UFe_2 are being studied intensively. For these, the experimental values of the maximal ΔE effect agree in order of magnitude with those calculated theoretically by Eq. (32), and they are very large. For the compound $TbFe_2$ it is 56% in fields up to 25 kOe at room temperature¹¹⁶ and reaches 60% in a 65-kOe field (at 210 K).¹¹⁷ The largest ΔE effect in rare-earth materials, which was 160%, has been found in one of the compounds with partially compensated anisotropy (see Sec. 7), $Tb_{0.3}Dy_{0.7}Fe_2$,¹¹⁸ Fig. 23.

The field-dependence of the ΔE effect is far harder to calculate than its maximal value. We note only that the "negative" ΔE effect known in $3d$ metals and alloys, i.e., the initial (in relatively small fields) decline in the Young's modulus of a material from that of the demagnetized state, has also been observed in the rare-earth compounds $TbFe_2$ ¹¹⁷ and $Tb_{0.20}Dy_{0.22}Ho_{0.58}Fe_2$.¹¹⁹ Here it is severalfold larger than, e.g., in the alloys of iron with cobalt.

A study of the phenomenon that is the thermodynamic inverse of the ΔE effect—a change in the magnetization ΔI (and magnetostriction) owing to external elastic compressive stresses has been performed on RFe_2

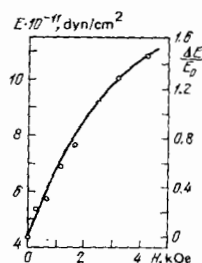


FIG. 23. Field dependence of the Young's modulus and the ΔE effect for the compound $Tb_{0.3}Dy_{0.7}Fe_2$ at room temperature.

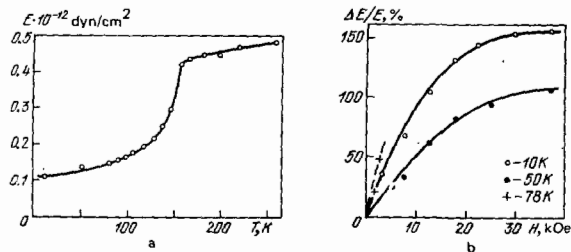


FIG. 24. a) Temperature-dependence of the Young's modulus of the intermetallic compound UFe_2 ; b) ΔE effect of the compound UFe_2 at the temperatures 10, 50, and 78 K.

polycrystals.^{120,121} It was noted that $\Delta I/I$ in $TbFe_2$ is even somewhat smaller (5% at 1 kG/mm²) than in nickel (6.9% and of opposite sign). Evidently the reason is that the rare-earth intermetallic material has considerably lower susceptibility than nickel. Yet even for $Tb_{0.3}Dy_{0.7}Fe_2$ the magnitude of $\Delta I/I$ amounts to 8% at 1 kG/mm². Beginning at a certain field value, the magnetostriction of these materials first decreases with increasing compressive load, and conversely, increases in large fields.

According to Eq. (32) a large susceptibility of the magnetization process, which corresponds, e.g., to a small value of the anisotropy energy, can lead to a considerable ΔE effect, even with a relatively small magnetostriction. As is known, it reaches 19% at ~500 K in annealed nickel.¹⁴ In the compound UFe_2 , as we have already noted above, a large magnetoelastic interaction is combined with a relatively small magnetic anisotropy. Therefore a large anomaly in the Young's modulus exists in this compound⁵⁶ (see Fig. 24a), and correspondingly an enormous ΔE effect: at 10 K the magnitude of E is increased by 160% as the field increases from zero to 35 kOe (Fig. 24b).

7. DYNAMIC PROPERTIES AND POSSIBLE APPLICATIONS OF MATERIALS SHOWING GIANT MAGNETOSTRICTION IN TECHNOLOGY

Most devices for technical purposes that use magnetostriction, e.g., for obtaining ultrasound, employ dynamic magnetostriction. A magnetostrictive material (a magnetostrictor) is placed in an alternating magnetic field, and such a device is one of the forms of a very simple electroacoustic transducer. Not only the large magnetostriction plays a role in the operation of the transducer, but also do other parameters that govern its acoustic potentialities. A method well known in acoustics of linearized equations has been developed to describe the operation of the transducer at relatively small amplitudes of magnetostriction.^{121,123} Let us present four of the eight such isothermal equations of state for a polycrystalline magnetostrictor^{124,126}:

$$\delta \epsilon = \left(\frac{\partial \epsilon}{\partial \sigma} \right)_H \delta \sigma + \left(\frac{\partial \epsilon}{\partial H} \right)_\sigma \delta H = \frac{1}{E_H} \delta \sigma + \frac{d}{4\pi} \delta H; \quad (33)$$

$$\delta B = \left(\frac{\partial B}{\partial \sigma} \right)_H \delta \sigma + \left(\frac{\partial B}{\partial H} \right)_\sigma \delta H = d \cdot \delta \sigma + \mu_\sigma \delta H; \quad (34)$$

$$\delta \sigma = \left(\frac{\partial \sigma}{\partial \epsilon} \right)_B \delta \epsilon + \left(\frac{\partial \sigma}{\partial B} \right)_\epsilon \delta B = E_B \delta \epsilon - h \delta B; \quad (35)$$

$$\delta H = \left(\frac{\partial H}{\partial \epsilon} \right)_B \delta \epsilon + \left(\frac{\partial H}{\partial B} \right)_\epsilon \delta B = -4\pi h \delta \epsilon + \frac{1}{\mu_\epsilon} \delta B. \quad (36)$$

The expansion of the thermodynamic functions describing the magnetic material is carried out in the variables B , H , σ , and ϵ (the induction and magnetic field intensity, the mechanical stress, and the relative strain); E_B is the Young's modulus at constant induction, i.e., without taking into account the magnetoelastic coupling (specimen with a short-circuited winding), and E_H is the same with account taken of the magnetoelastic interaction; μ_σ and μ_ϵ are the magnetic susceptibilities of a free and of a clamped specimen. The magnetostrictive constant

$$h = - \left(\frac{\partial \sigma}{\partial B} \right)_\epsilon = - \frac{1}{4\pi} \left(\frac{\partial H}{\partial \epsilon} \right)_B \quad (37)$$

(the latter equation stems from thermodynamic considerations) and the sensitivity constant (of a magnetostrictor as an acoustic receiver)

$$d = \left(\frac{\partial B}{\partial \sigma} \right)_H = 4\pi \left(\frac{\partial \epsilon}{\partial H} \right)_\sigma \quad (38)$$

are the two most important acoustic constants. Equation (38) corresponds to the relationship (4) presented above. One can express the quantity h (for the ideal case of hysteresis-free magnetostriction) as

$$h = \frac{E_B}{\mu_B} \frac{\partial \lambda}{\partial H}. \quad (39)$$

That is, an essential requirement on the material is a very steep slope of the (static) magnetostriction curve $\lambda(H)$ (or a small value of the magnetic anisotropy constant). The choice of the best "working point" on this curve, and above all, the operation of the transducer at the frequency of the current supplying the coil, rather than at the doubled frequency (magnetostriction is an even effect) require a constant magnetic biasing field having the induction B_0 , as well as an alternating magnetic induction with the amplitude B . [which we can consider equal to δB in Eqs. (33)–(36)]. Here the magnetic material becomes a magnetically polarized medium, i.e., transversely isotropic.

Strictly speaking, one can employ Eqs. (33)–(36) only at small $B < B_0$. As the amplitude of the variables entering into these equations is increased, nonlinearities arise in the magnetostrictive vibrations, which can be taken into account by taking the higher-order terms in the expansions of the thermodynamic functions, or by assuming that the dynamic coefficients h , d (and others) depend on B .

Another very important parameter of a magnetostrictive acoustic transducer is the magnetomechanical coupling coefficient k . It can be determined by the equation

$$k^2 = \frac{W_{\text{elast}}}{W_{\text{magn}}}. \quad (40)$$

Here W_{elast} is the magnitude of the converted (elastic) energy arising in the transducer when magnetically excited, and W_{magn} is the ("input") energy of the corresponding magnetic field. The coupling coefficient k characterizes the efficiency of conversion in the given device of the one type of energy into the other (involving, e.g., the unavoidable reactive return of part of the

“input” energy to its source) without taking into account radiation and magnetic and mechanical losses.

In turn, these losses are taken into account by introducing the acoustic efficiency of the transducer, $\eta = P_{\text{acoust}}/P_{\text{electr}}$, i.e., the ratio of the acoustic power supplied at the output to the electric power consumed at the input. The quantity η depends on the properties of the transducer itself, on its shape, on the ratio of its dimensions to the emitted wavelength, and to a certain degree, on the wave resistance of the “load”—the medium surrounding the transducer, which is ρv , where ρ is the density of the medium, and v is the velocity of sound in it.⁶ The limiting potentialities of the transducer material involve its strength and the maximum density of elastic energy in it, i.e., the quantity $\lambda_s^2 E/2$, where λ_s is the saturation magnetostriction. At a constant value of λ_s , much will be determined by the Young’s modulus E of the material. Moreover, the magnitude of the ΔE effect of the material will be important. This affects the displacement of the resonance frequency of the mechanical (most often longitudinal) vibrations of the transducer as the value of the induction B_0 of the magnetic biasing field is changed.

The amplitude of the deformations of the transducer depends also on its mechanical Q factor. The latter, i.e., the internal friction in the material without allowing for the effect of the magnetic field, is also involved with a certain fraction of the heat losses in the transducer. In turn, the main reasons for these losses (now in the presence of the field) are its induction currents and magnetic hysteresis. The losses in eddy currents depend on the value of the resistivity and the geometry of the specimen of material, while the magnetic hysteresis losses depend mainly on the magnitude of the coercive forces.

These are the fundamental parameters, though far from all, that characterize a magnetostrictive transducer. Let us briefly examine the potentialities of materials having giant magnetostriction and certain ways of improving their properties.

The potentialities of applying the giant magnetostriction of the pure rare-earth metals, their alloys with one another, and of such interesting actinide compounds as UFe_2 are as yet strongly restricted by their Curie points, which lie considerably below room temperature. Therefore we shall mainly discuss below the materials of the RFe_2 type.

As a rule, if the topic is applications, there is no point in speaking of the saturation magnetostriction λ_s of polycrystals of these materials, since it is reached in fields too large for practice, sometimes of the order of 100 kOe or more. Therefore the question is usually that of the magnitude of the longitudinal λ_{\parallel} (or “total” $\lambda_{\parallel} - \lambda_{\perp}$) magnetostriction in a fixed external field of 12–25 kOe, and of the maximum value of the quantity $\partial\lambda/\partial H$, which involves the magnetostrictive dynamic constant h , cf. Eqs. (37) and (38). The compound TbFe_2 possesses the largest magnetostriction of all the binary compounds of the RFe_2 type.³¹ Depending on the conditions of preparation, the value of λ_{\parallel} in a 15-kOe field

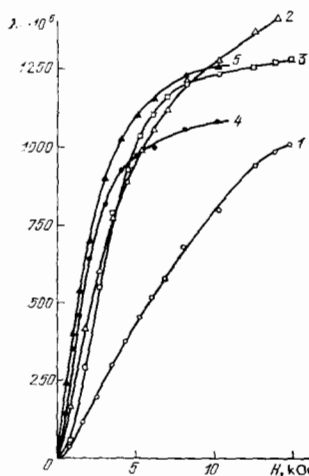


FIG. 25. Field-dependences of the longitudinal magnetostriction of some RFe_2 -type compounds at room temperature. 1— TbFe_2 ; 2—textured TbFe_2 ; 3— $\text{Tb}_{0.27}\text{Dy}_{0.73}\text{Fe}_2$; 4—a compound of the system $(\text{Tb-Dy-Er})\text{Fe}_2$; 5—a compound of the system $(\text{Tb-Dy-Ho})\text{Fe}_2$.

for it amounts to $(1000-1200) \times 10^{-6}$ and $(200-360) \times 10^{-6}$ at 2 kOe, while $(\partial\lambda/\partial H)_{\text{max}}$ is equal on the average to $13 \times 10^{-8} \text{ Oe}^{-1}$ (Fig. 25, curve 1). Partial replacement of terbium or iron in this compound with other metals yields no significant effect.^{90,105,127,128} For textured (oriented) specimens of TbFe_2 prepared by a special technique, the magnetostriction in a 15-kOe field reaches $\lambda_{\parallel} \geq 1500 \times 10^{-6}$ (Fig. 25, curve 2). Such considerable fields required to realize $\lambda \sim 10^{-3}$ are necessary because of the large magnetocrystalline anisotropy of these compounds (for TbFe_2 , $K_1 = -7.6 \times 10^7 \text{ erg/cm}^3$ at room temperature¹²⁹).

One of the most important ways of perfecting magnetostrictive materials is to increase the quantity $\partial\lambda/\partial H$ mentioned above. This is almost equivalent to reducing their anisotropy constants K_1 and K_2 . In this connection, we present Table X, which gives the signs of λ_{\parallel} , K_1 , and K_2 for certain of the most important compounds.³⁷

Upon taking into account the single-ion character of the magnetic anisotropy and the magnetostriction, one can obtain a large value of λ with a small value of K_1 in intermetallic substances of the complex composition $\text{R}_x\text{R}'_{1-x}\text{Fe}_2$ if the signs of the magnetostriction are the same in the “starting” compounds, while the signs of the constants K_1 differ. Such compounds are $\text{Tb}_{0.3}\text{Dy}_{0.7}\text{Fe}_2$,¹³⁰ and $\text{Tb}_{0.15}\text{Ho}_{0.85}\text{Fe}_2$.⁹² The dependence

TABLE X. Signs of the longitudinal magnetostriction and of the anisotropy constants of RFe_2 compounds.

	PrFe_2 *	SmFe_2	TbFe_2	DyFe_2	HoFe_2	ErFe_2	TmFe_2	YbFe_2 *
λ_{\parallel}	+	—	+	+	+	—	—	—
K_1	+	—	—	+	+	—	—	+
K_2	—	0	—	—	+	—	+	—

*Not actually synthesized.

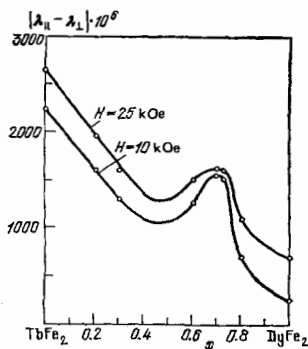


FIG. 26. Concentration-dependences of the overall magnetostriction ($\lambda_{11} - \lambda_1$) of compounds of the system $Tb_{1-x}Dy_xFe_2$ in fields of 10 and 25 kOe at room temperature.

of λ on the dysprosium concentration for compounds of the system $Tb_{1-x}Dy_xFe_2$ is shown in Fig. 26, in which we see the corresponding maximum of λ near $x = 0.7$. In the magnetic-orientational phase diagrams, the given compositions lie near the lines of spin-reorientation transitions.⁷ For example, the compound $Tb_{0.3}Dy_{0.7}Fe_2$ or the similar $Tb_{0.27}Dy_{0.73}Fe_2$ ("terfenol"), which has been used in a number of studies, lie at room temperature in the region of the diagram (see Fig. 21) where the axis of easy magnetization in the crystal lies along $\langle 111 \rangle$, but rotates toward the direction $\langle 100 \rangle$ below 280 K. Here K_1 declines sharply from values $10^7 - 10^6$ erg/cm³ to 10^4 erg/cm³, since the anisotropy energy is partially compensated by the large magnetostrictive contribution.^{110, 131}

However, the value of $\partial\lambda/\partial H = (25 - 30) \times 10^{-8}$ Oe⁻¹ (see Fig. 25, curve 3) thus obtained is not a record-setting value, since the second anisotropy constants here do not compensate. The search for compounds with larger $\partial\lambda/\partial H$ is being conducted by using compounds containing three rare-earth elements. A calculation by the method presented in Ref. 132, which requires knowing the first anisotropy constants of the binary compound (they have been given in Refs. 133 and 134) yields straight lines in the concentration triangle corresponding to $K_1 = 0$ for the "overall" compound. Upon varying the compositions near this straight line, one can also experimentally minimize the value of the second anisotropy constant K_2 . By this method one can obtain compounds of the systems (Tb-Dy-Ho)Fe₂ and (Tb-Dy-Er)Fe₂ for which $\partial\lambda/\partial H \approx 50 \times 10^{-8}$ Oe⁻¹ (see Fig. 25, curves 4 and 5). A set of other "quaternary" compounds of similar type has also been found, both with positive^{37, 38} magnetostriction, e.g., $Tb_{0.20}Dy_{0.22}Ho_{0.58}Fe_2$, which has $\lambda_s = 530 \times 10^{-6}$ and a considerable $\partial\lambda/\partial H$,¹³⁵ and with negative magnetostriction (based on samarium).¹³⁶

The problem of increasing $\partial\lambda/\partial H$ might be solved most simply by using singlecrystals of the corresponding intermetallic materials, but growing them is impossible in some cases, and presents considerable difficulty in others. For the $TbFe_2$ crystal with the magnetostriction along the axis of easy magnetization we have $\partial\lambda_{111}/\partial H = 120 \times 10^{-8}$ Oe⁻¹,¹²⁹ and for $Tb_{0.27}Dy_{0.73}Fe_2$ it is $\sim 110 \times 10^{-8}$ Oe⁻¹ at room temperature¹³⁷ (see Fig.

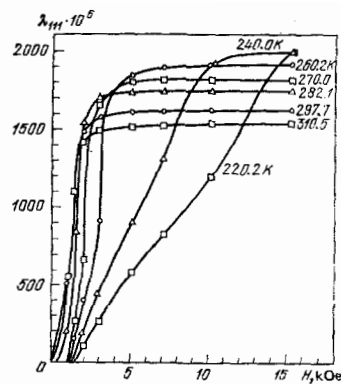


FIG. 27. Field-dependence of the magnetostriction along the $\langle 111 \rangle$ axis of a single crystal of the compound $Tb_{0.27}Dy_{0.73}Fe_2$ at temperatures from 220.2 to 310.5 K.

27). A set of studies on single crystals and the method of growing one of these systems are described in Refs. 38, 131, and 138.

Another index very important for an acoustic transducer, the magnetomechanical coupling coefficient k , is generally larger whenever $\partial\lambda/\partial H$ is larger. Measurements (with an open magnetic flux) on $TbFe_2$ have yielded $k \approx 0.20$,¹³⁹ i.e., about the same as for the traditional magnetostrictive material nickel. Compounds with compensated anisotropy (in measurements with a closed magnetic flux) show, also in air, higher values of the coupling coefficient: for $Tb_{0.27}Dy_{0.73}Fe_{2-\delta}$ ($\delta = 0.02 - 0.05$) its value in different magnetic biasing fields varies over a range from 0.3 to 0.6,¹¹⁶ while $Tb_{0.145}Ho_{0.855}Fe_2$ has $k_{max} = 0.34$.¹⁴⁰ The magnetic biasing field H_0 in these materials is considerably larger than in nickel, but the function $k(H_0)$ shows a broad maximum, whereas for nickel this maximum is sharp. That is, one must keep the value of H_0 strictly fixed to obtain k_{max}^N . Table XI compares the acoustic parameters of one of the rare-earth magnetostrictive materials with the traditional materials and with a piezoceramic. We note that the specimens, as yet unique, of polycrystals with oriented grains show the record-setting value of $k = 0.74$.¹⁴² This is larger than for the piezoceramic, while alloys that lie on the verge of the transition of the axis of easy magnetization from the $\langle 111 \rangle$ direction to $\langle 100 \rangle$ yield a value of k almost invariant from 293 to 363 K.^{131, 143} The mechanical Q factors of specimens of these materials lie in the range from 70 to 200.¹¹⁶

These are the fundamental acoustic parameters of the metallic rare-earth magnetostrictive materials. As we have already mentioned, certain of their other characteristics also play a substantial role in technical applications. These include the parameters of the magnetic hysteresis loop (magnetization, coercive force, differential magnetic susceptibility), the resistivity, and certain others. Data on them are given in Refs. 90 and 130. By using them, one can estimate the heat losses in dynamic remagnetization (in specimens of magnetostrictive materials obtained by different meth-

TABLE XI. Dynamical properties of certain piezomaterials.

Material	Maximum coupling coefficient k	Density of electromechanical energy (for optimal values of the constant and alternating fields) $w, \text{J/m}^3$	Acoustic efficiency $\eta, \%$	References
Nickel	0.3	21	15	140
Permendur K49F2	0.35	40		141
Piezoceramic RZT-4	0.7	670	70	140
$\text{Tb}_{0.27}\text{Dy}_{0.73}\text{Fe}_2$	0.6	5300		140

ods), which arise mainly from losses in magnetic hysteresis, which increase linearly with the frequency, and from losses in induction currents, which are known to be proportional to the square of the frequency. The dynamic losses can be diminished by a considerable decrease in the coercive force, as in oriented crystals, and by increasing the electric resistance. The strength of RFe_2 polycrystals is not sufficient, especially for impact loads. One also cannot roll the brittle intermetallic compounds, while the problem of cutting specimens into thin plates (so as to prepare transducer cores similar to transformer cores) is not simple, owing to their great hardness.

One of the promising methods here is metalloceramic technology,^{90,144,145} with which one can prepare magnetostrictors of any shape and dimensions. They are substantially more durable, they do not corrode, and their electric resistance is also higher than for the cast materials. However, the magnetostriction is somewhat smaller, e.g., the metalloceramic of $\text{Tb}_{0.3}\text{Dy}_{0.7}\text{Fe}_2$ has $\lambda_{11} = 860 \times 10^{-6}$ in a 17-kOe field.¹⁴⁴

However, one can increase the value of the striction by pressing the part (before sintering it) in a magnetic field, i.e., obtaining an oriented metalloceramic,^{146,147} as in preparing permanent magnets of the SmCo_5 type. Since $\lambda_{111} \gg \lambda_{100}$ for these materials, in line with Eq. (3), the orientation of the particles of the powder along the axis of easy magnetization $\langle 111 \rangle$ substantially increases the striction (Fig. 28).

Metalloceramic technology is not the only way of preparing new magnetostrictive materials applicable in practice. In particular, studies are being conducted on amorphous materials. For example, an overall

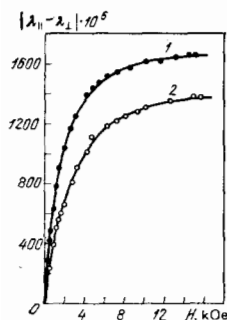


FIG. 28. Field-dependences of the overall magnetostriction of specimens of $\text{Tb}_{0.3}\text{Dy}_{0.7}\text{Fe}_2$ prepared by metalloceramic technology. Curve 1—for the compound obtained by orienting the particles in a 20-kOe field in the initial pressing; 2—obtained by “liquid-phase” sintering (without a field).

striction $\lambda_{11} - \lambda_{10} = 450 \times 10^{-6}$ has been attained in a 25-kOe field in amorphous TbFe_2 .³⁷

A number of studies^{148,149} has already described trial designs of magnetostrictive transducers, e.g., made from rods of metalloceramic terfenol. The rods in these designs are sometimes subjected to compressive stress, which increases their strength. The supply of large currents to such devices—magnetic biasing and ac at the required frequency—is a definite technical problem, and the maximal density of elastic energy, which is proportional to λ_s^2 , has not yet been attained in them. One of their advantages is the possibility of employment as broad-band, or even nonresonance, transducers.

There are many fields of technology where the application of giant magnetostriction can produce a substantial effect. At room temperature, this is primarily in the applications that do not require prolonged, constant operation of the transducer, and pulsed regimes can be employed, while one requires at the same time a considerable rigidity of the element that changes in length (or other dimensions). These are ring or rod magnetostrictors, which can be applied in logging of drill holes or for “sounding” between drill holes in geophysical prospecting; various contactors, relays, stepping motors in automation and remote control, and many others. After solving a number of problems involving reducing the losses in cores operating under conditions of dynamic magnetostriction, these will become varied, powerful emitters of sound and ultrasound. They can be applied for purposes of defectoscopy, cleaning, and precipitation, fine, grain crystallization of metals, comminution, cutting, etc. When low (liquid-nitrogen) temperatures can be used, one can employ as magnetostrictive materials a broader set of rare-earth metals, their alloys with one another, and uranium compounds.

8. CONCLUSION

In this review we have tried to summarize the fundamental results of the experimental and theoretical studies of giant magnetostrictive effects in compounds of the rare earths and actinides.

We have shown that these effects are of single-ion type and arise from the interaction of the anisotropic cloud of f -electrons with the crystal field of the lattice (“rigid” electron-cloud model). We have analyzed the conditions for appearance of giant magnetostriction in different types of magnetic materials. We have discussed the influence of the magnetoelastic interaction on the magnetic anisotropy and elastic properties of the rare earths and actinides.

In order to elucidate the prospects of technical application, we have described certain features of the manifestation of giant magnetostriction in alternating magnetic fields, and presented the fundamental parameters characterizing the efficiency of operation of magnetostrictive transducers.

At present one of the most important fields in the study of giant magnetostriction is the creation of a microscopic theory of the magnetostriction of the rare-earth and actinide magnetics. Creation of such a theory would enable a goal-directed search for new magnetostrictive materials and prediction of their properties.

We note that in this review we have mainly treated the anisotropic magnetostriction of the rare-earth and actinide magnetic materials. We have not treated at all other magnetoelastic phenomena in rare-earth and actinide magnetic materials, or have discussed them in lesser detail (only to the degree necessary for elucidating the features and nature of anisotropic magnetostriction). These phenomena are of independent scientific interest, such as, e.g., the anomalous behavior of the thermal expansion coefficient (invar effect¹⁵⁰⁻¹⁵²), helicoidal magnetostriction,^{11,153} magnetic anomalies of "non-domain" type in the elastic moduli and internal friction,^{154,155} and a number of others.

Also a broad set of phenomena has fallen outside the scope of the review that arise from the dynamics of the magnetoelastic interaction of the magnetic and elastic subsystems of crystals. As we see it, this problem merits separate treatment.

Speaking of possible technical applications, we should mention in addition, in particular, magnetic-field-controlled acoustic delay lines, which are made possible by the large ΔE effect of crystals showing giant magnetostriction.¹⁵⁶

We feel that the conclusion from this review as a whole is that the problem of giant magnetostriction is highly interesting, both in the theoretical and practical aspects.

¹J. P. Joule, *Philos. Mag.* **30**, 76, 225 (1847).

²S. V. Vonsovskii, *Magnetizm (Magnetism)*, Nauka, M., 1971.

³K. P. Belov, *Uprugie, teplovye i elektricheskie yavleniya v ferromagnetikakh (Elastic, Thermal, and Electric Phenomena in Ferromagnetics)*, Gostekhizdat, M., 1957.

⁴E. I. Kondorskiĭ and V. L. Sedov, *Zh. Eksp. Teor. Fiz.* **35**, 845, 1579 (1958); **38**, 773 (1960) [*Sov. Phys. JETP* **8**, 586, 1104 (1959); **11**, 561 (1960)].

⁵N. P. Grazhdankina, *Usp. Fiz. Nauk* **96**, 291 (1968) [*Sov. Phys. Usp.* **11**, 727 (1969)].

⁶E. V. Kuz'min, G. A. Petrakovskii, and É. A. Zavadskii, *Fizika magnitoporyadochennykh veshchestv (Physics of Magnetically Ordered Materials)*, Nauka, Novosibirsk, 1976.

⁷K. P. Belov, A. K. Zvezdin, A. M. Kadomtseva, and R. Z. Levitin, *Magnitnye orientatsionnye perekhody v redkozemel'nykh magnetikakh (Magnetic Orientational Transitions in Rare-Earth Magnetics)*, Nauka, M., 1979.

⁸I. P. Golyamina, ed., *Ul'trazvuk: Malen'kaya éntsiklopediya (Ultrasound: Small Encyclopedia)*, *Sov. Entsiklopediya*, M., 1979.

⁹K. P. Belov, R. Z. Levitin, and S. A. Nikitin, in: *Tezisy dokladov na soveshchanii po ferromagnetizmu i antiferro-*

magnetizmu (Abstracts of Papers at the Conference on Ferromagnetism and Antiferromagnetism), *Izd-vo AN SSSR*, L., 1961, p. 90.

¹⁰K. P. Belov, R. Z. Levitin, and S. A. Nikitin, *Fiz. Met. Metalloved.* **11**, 948 (1961).

¹¹K. P. Belov, M. A. Belyanchikova, S. A. Nikitin, and R. Z. Levitin, *Redkozemel'nye ferro- i antiferromagnetiki (Rare-Earth Ferro- and Antiferromagnetics)*, Nauka, M., 1965.

¹²K. P. Belov, *Redkozemel'nye magnetiki i ikh primenenie (Rare-Earth Magnetic Materials and Their Applications)*, Nauka, M., 1980.

¹³Ch. Kittel, in: *Fizika ferromagnitnykh oblastei (Physics of Ferromagnetic Regions)*, IL, M., 1951.

¹⁴R. M. Bozorth, *Ferromagnetism*, Van Nostrand, New York, 1951 (Russ. Transl., IL, M., 1956).

¹⁵K. P. Belov, R. Z. Levitin, S. A. Nikitin, and A. V. Ped'ko, *Zh. Eksp. Teor. Fiz.* **40**, 1562 (1961) [*Sov. Phys. JETP* **13**, 1096 (1961)].

¹⁶K. P. Belov and S. A. Nikitin, *ibid.* **42**, 403 (1962) [*Sov. Phys. JETP* **15**, 279 (1962)].

¹⁷E. Lee and L. Alberts, *Proc. Phys. Soc. London* **79**, 997 (1962).

¹⁸S. A. Nikitin, *Zh. Eksp. Teor. Fiz.* **43**, 31 (1962) [*Sov. Phys. JETP* **16**, 21 (1963)].

¹⁹R. Z. Levitin, *Abstract of doctoral dissertation*, Moscow State University, M., 1973.

²⁰A. Clark, B. De Savage, and R. Bozorth, *Phys. Rev.* **138**, 216 (1965).

²¹S. Legvold, J. Alstad, and J. Rhyne, *Phys. Rev. Lett.* **10**, 509 (1963).

²²R. Z. Levitin, Yu. F. Popov, and O. D. Chistyakov, *Pis'ma Zh. Eksp. Teor. Fiz.* **16**, 222 (1972) [*JETP Lett.* **16**, 157 (1972)].

²³S. A. Nikitin, *Zh. Eksp. Teor. Fiz.* **80**, 207 (1981) [*Sov. Phys. JETP* **53**, 104 (1981)].

²⁴Kh. Bartolin, in: *Redkozemel'nye metally, splavy i soedineniya (Rare-Earth Metals, Alloys, and Compounds)*, Nauka, M., 1973, p. 125.

²⁵R. Aleonard, P. Boutron, and D. Bloch, *J. Phys. Chem. Solids* **30**, 2277 (1969).

²⁶J. Alstad and S. Legvold, *J. Appl. Phys.* **35**, 1752 (1964).

²⁷J. Rhyne and S. Legvold, *Phys. Rev.* **138**, A507 (1965).

²⁸K. P. Belov, R. Z. Levitin, and B. K. Ponomarev, *Zh. Eksp. Teor. Fiz.* **49**, 1733 (1965) [*Sov. Phys. JETP* **22**, 1185 (1966)].

²⁹K. P. Belov, S. A. Nikitin, N. A. Sheludko, V. P. Posyado, and G. E. Chuprikov, *ibid.* **73**, 270 (1977) [*Sov. Phys. JETP* **46**, 140 (1977)].

³⁰V. A. Finkel', *Struktura redkozemel'nykh metallov (Structure of the Rare-Earth Metals)*, *Metallurgiya*, M., 1978.

³¹N. Koon, A. Schindler, and F. Carter, *Phys. Lett. A* **37**, 413 (1971).

³²B. Barbara, J. P. Girard, J. Laforest, R. Lemaire, E. Siaud, and J. Schweizer, *Physica (Utrecht) Ser. B* **86-88**, 155 (1977).

³³A. S. Markosyan, *Fiz. Tverd. Tela (Leningrad)* **22**, 3454 (1980) [*Sov. Phys. Solid State* **22**, 2023 (1980)].

³⁴A. S. Markosyan, *ibid.* **23**, 1153 (1981) [*Sov. Phys. Solid State* **23**, 670 (1981)].

³⁵A. S. Markosyan, *ibid.* **23**, 1656 (1981) [*Sov. Phys. Solid State* **23**, 965 (1981)].

³⁶S. Siaud and J. Schweizer, *Physica (Utrecht) Ser. B* **86-88**, 255 (1977).

³⁷A. E. Clark, in: *Handbook on the Physics and Chemistry of Rare Earths*, eds. K. A. Gschneider, Jr. and I. Eyring, North-Holland, Amsterdam, 1979, Chap. 15, p. 231.

³⁸A. E. Clark, R. Abbundi, H. T. Savage, and O. D. McMasters, *Physica (Utrecht) Ser. B* **86-88**, 73 (1977).

³⁹A. V. Andreev, A. V. Deryagin, S. M. Zadvorskiĭ, and V. N.

- Moskalev, *Fiz. Met. Metalloved.* **51**, 975 (1981).
- ⁴⁰R. Abbundi, A. E. Clark, and N. C. Koon, *J. Appl. Phys.* **50**, 1671 (1979).
- ⁴¹R. Abbundi and A. E. Clark, *ibid.* **49**, 1969 (1978).
- ⁴²K. P. Belov and V. I. Sokolov, *Zh. Eksp. Teor. Fiz.* **48**, 979 (1965) [*Sov. Phys. JETP* **21**, 652 (1965)].
- ⁴³V. I. Sokolov and T. D. Khien, *ibid.* **52**, 1485 (1967) [*Sov. Phys. JETP* **25**, 986 (1967)].
- ⁴⁴A. E. Clark, B. F. De Savage, N. Tsuja, and S. Kawakami, *J. Appl. Phys.* **37**, 1324 (1966).
- ⁴⁵A. E. Clark, J. J. Rhyne, and E. R. Callen, *J. Appl. Phys.* **39**, Part 1, 573 (1978).
- ⁴⁶S. Iida, *J. Phys. Soc. Jpn.* **22**, 1201 (1967).
- ⁴⁷E. R. Callen, A. E. Clark, B. F. De Savage, and W. Coleman, *Phys. Rev.* **130**, 1735 (1963).
- ⁴⁸V. P. Kiryukhin and V. I. Sokolov, *Zh. Eksp. Teor. Fiz.* **51**, 428 (1966) [*Sov. Phys. JETP* **24**, 287 (1967)].
- ⁴⁹K. P. Belov, V. P. Kiryukhin, and V. I. Sokolov, *Pis'ma Zh. Eksp. Teor. Fiz.* **3**, 329 (1966) [*JETP Lett.* **3**, 212 (1966)].
- ⁵⁰F. Sayetat, *J. Appl. Phys.* **46**, 3619 (1975).
- ⁵¹V. Tshebyatovskii, Z. Genke, K. P. Belov, A. S. Dmitrievskii, R. Z. Levitin, and Yu. F. Popov, *Zh. Eksp. Teor. Fiz.* **61**, 1522 (1971) [*Sov. Phys. JETP* **34**, 811 (1972)].
- ⁵²K. P. Belov, Z. Genke, A. S. Dmitrievskii, Z. Zygmunt, R. Z. Levitin, and Yu. F. Popov, in: *Trudy mezhdunarodnoi konferentsii po magnetizmu* (Proceedings of the International Conference on Magnetism), Nauka, M., 1974, Vol. 6, p. 54.
- ⁵³C. Sampson, F. Wedgwood, and N. Satya-Murthy, *J. Phys.* **C 9**, 4035 (1976).
- ⁵⁴R. Z. Levitin, A. S. Dmitrievskii, Z. Henke, and A. Misiuk, *Phys. Status Solidi A* **27**, K109 (1975).
- ⁵⁵A. V. Andreev, K. P. Belov, A. V. Deryagin, Z. A. Kazei, R. Z. Levitin, Yu. F. Popov, and V. I. Silant'ev, *Zh. Eksp. Teor. Fiz.* **75**, 2351 (1978) [*Sov. Phys. JETP* **48**, 1187 (1978)].
- ⁵⁶Yu. F. Popov, R. Z. Levitin, M. Zeleny, A. V. Deryagin, and A. V. Andreev, *ibid.* **78**, 2431 (1980) [*Sov. Phys. JETP* **51**, 1223 (1980)].
- ⁵⁷J. Marples, *J. Phys. Chem. Solids* **31**, 2431 (1970).
- ⁵⁸J. Marples, C. Sampson, and F. Wedgwood, *J. Phys.* **C 8**, 708 (1975).
- ⁵⁹G. H. Lander and M. H. Muller, *Phys. Rev. B* **10**, 1934 (1974).
- ⁶⁰A. T. Aldred, B. D. Dunlap, A. R. Harvey, D. J. Lam, G. H. Lauder, and M. H. Mueller, *Phys. Rev. B* **9**, 3766 (1974).
- ⁶¹M. Mueller, C. Lauder, H. Hoff, H. Knott, and J. Reddy, *J. Phys. (Paris)* **40**, C4-68 (1979).
- ⁶²J. Rossat-Mignod, P. Burdt, S. Quezel, and O. Vogt, *Physica (Utrecht) Ser. B* **102**, 237 (1980).
- ⁶³E. Fawcett and G. K. White, *J. Appl. Phys.* **39**, Part 1, 576 (1968).
- ⁶⁴P. L. Kapitza, *Proc. R. Soc. London* **135**, 568 (1932).
- ⁶⁵K. P. Belov and V. N. Sokolov, *Pis'ma Zh. Eksp. Teor. Fiz.* **4**, 186 (1966) [*JETP Lett.* **4**, 127 (1966)].
- ⁶⁶K. P. Belov, V. I. Sokolov, and T. D. Khien, *Fiz. Tverd. Tela (Leningrad)* **10**, 3706 (1968) [*Sov. Phys. Solid State* **10**, 2946 (1969)].
- ⁶⁷T. V. Valyanskaya and V. I. Sokolov, *ibid.* **18**, 297 (1976) [*Sov. Phys. Solid State* **18**, 175 (1976)].
- ⁶⁸L. A. Bumagina, V. I. Krotov, B. Z. Malkin, and A. Kh. Khasanov, *Zh. Eksp. Teor. Fiz.* **80**, 1543 (1981) [*Sov. Phys. JETP* **53**, 792 (1981)].
- ⁶⁹S. A. Al'tshuler, F. L. Aukhadeev, V. A. Grevtsev, and M. A. Teplov, *Pis'ma Zh. Eksp. Teor. Fiz.* **22**, 159 (1975) [*JETP Lett.* **22**, 73 (1975)].
- ⁷⁰I. V. Aleksandrov, L. G. Mamsurova, K. K. Pukhov, N. G. Trusevich, and L. G. Shcherbakova, *ibid.* **34**, 68 (1981) [*JETP Lett.* **34**, 68 (1981)].
- ⁷¹K. P. Belov, *Vestn. MGU, Ser. III, No. 5*, 23 (1967).
- ⁷²N. Tsuya, A. Clark, and R. Bozorth, in: *Proc. Intern. Conference on Magnetism*, Nottingham, 1964, p. 250.
- ⁷³J. Slonczewski, *J. Appl. Phys.* **32**, 253S (1961).
- ⁷⁴E. A. Turov, *Fizicheskie svoystva magnituporyadochennykh kristallov* (Physical Properties of Magnetically Ordered Crystals), Izd-vo AN SSSR, M., 1963, p. 224.
- ⁷⁵N. S. Akulov, *Ferromagnetizm* (Ferromagnetism) (Eng. Transl., Academic Press, New York, 1965), Gostekhizdat, M., L., 1939, p. 188.
- ⁷⁶W. Mason, *Phys. Rev.* **96**, 302 (1954).
- ⁷⁷E. Callen and H. Callen, *ibid.* **129**, 578 (1963).
- ⁷⁸E. Callen and H. Callen, *ibid.* **139**, 455 (1965).
- ⁷⁹C. Kittel and J. Van Vleck, *Phys. Rev.* **118**, 1231 (1960).
- ⁸⁰E. A. Turov and A. I. Mitsek, *Zh. Eksp. Teor. Fiz.* **38**, 1847 (1960) [*Sov. Phys. JETP* **11**, 1327 (1960)].
- ⁸¹R. Z. Levitin, E. M. Savitskii, V. F. Terekhova, O. D. Chistyakov, and V. L. Yakovenko, in: *Splavy redkozemel'nykh metallov s osobymi fizicheskimi svoystvami* (Alloys of Rare-Earth Metals with Special Physical Properties), Nauka, M., 1974, p. 100.
- ⁸²S. A. Nikitin, D. Kim, and O. D. Chistyakov, *Zh. Eksp. Teor. Fiz.* **71**, 1610 (1976) [*Sov. Phys. JETP* **44**, 843 (1976)].
- ⁸³S. A. Nikitin, A. S. Andreev, V. P. Posyado, and G. E. Chuprikov, *Fiz. Tverd. Tela (Leningrad)* **19**, 1792 (1977) [*Sov. Phys. Solid State* **19**, 1045 (1977)].
- ⁸⁴S. A. Nikitin, N. A. Sheludko, V. P. Posyado, and G. E. Chuprikov, *Zh. Eksp. Teor. Fiz.* **73**, 1001 (1977) [*Sov. Phys. JETP* **46**, 530 (1977)].
- ⁸⁵K. P. Belov, E. M. Savitskii, V. F. Terekhova, S. A. Nikitin, S. M. Nakvi, and O. D. Chistyakov, in: *Splavy redkikh i tugoplavkikh metallov s osobymi fizicheskimi svoystvami* (Alloys of Rare and Refractory Metals with Special Physical Properties), Nauka, M., 1979, p. 121.
- ⁸⁶S. A. Nikitin and N. P. Arutyunyan, *Zh. Eksp. Teor. Fiz.* **77**, 2018 (1979) [*Sov. Phys. JETP* **50**, 962 (1979)].
- ⁸⁷H. Child, W. Koehler, E. Wollan, and J. Cable, *Phys. Rev.* **138**, 1655 (1965).
- ⁸⁸S. A. Nikitin, *Zh. Eksp. Teor. Fiz.* **77**, 343 (1979) [*Sov. Phys. JETP* **50**, 176 (1979)].
- ⁸⁹I. E. Dzyaloshinskii, *Zh. Eksp. Teor. Fiz.* **47**, 336 (1964) [*Sov. Phys. JETP* **20**, 223 (1965)].
- ⁹⁰K. P. Belov, E. P. Bochkarev, K. I. Epifanova, G. I. Kataev, D. Kim, S. A. Nikitin, Yu. F. Popov, and G. E. Chuprikov, *Fiz. Met. Metalloved.* **43**, 295 (1977).
- ⁹¹A. Clark, J. Callen, O. McMasters, and E. Callen, *AIP Conf. Proc.*, No. 29, 192 (1976).
- ⁹²N. Koon, A. Schindler, C. Williams, and F. Carter, *J. Appl. Phys.* **45**, 5389 (1974).
- ⁹³S. A. Nikitin and A. M. Bisliiev, *Fiz. Tverd. Tela (Leningrad)* **15**, 3681 (1973) [*Sov. Phys. Solid State* **15**, 2451 (1974)].
- ⁹⁴E. Burzo, *Solid State Commun.* **14**, 1295 (1974).
- ⁹⁵E. Callen and H. Callen, *Phys. Rev.* **129**, 578 (1963).
- ⁹⁶P. Flanders, R. Pearson, and J. Page, *Br. J. Appl. Phys.* **17**, 839 (1966).
- ⁹⁷K. P. Belov, A. K. Gapeev, R. Z. Levitin, A. S. Markosyan, and Yu. F. Popov, *Zh. Eksp. Teor. Fiz.* **68**, 241 (1975) [*Sov. Phys. JETP* **41**, 117 (1975)].
- ⁹⁸N. M. Kolacheva, R. Z. Levitin, B. V. Mill', and L. P. Shlyakhina, *Fiz. Tverd. Tela (Leningrad)* **18**, 3625 (1976) [*Sov. Phys. Solid State* **18**, 2111 (1976)].
- ⁹⁹N. M. Kolacheva, R. Z. Levitin, B. V. Mill', and L. P. Shlyakhina, *ibid.* **21**, 1038 (1979) [*Sov. Phys. Solid State* **21**, 604 (1979)].
- ¹⁰⁰K. P. Belov, *Ferrity v sil'nykh magnitnykh polaykh* (Ferrites in Strong Magnetic Fields), Nauka, M., 1972.
- ¹⁰¹R. Z. Levitin, B. K. Ponomarev, and Yu. F. Popov, *Zh. Eksp. Teor. Fiz.* **59**, 1952 (1970) [*Sov. Phys. JETP* **32**, 1056 (1971)].
- ¹⁰²S. A. Al'tshuler, S. S. Krotov, and B. Z. Malkin, *Pis'ma Zh. Eksp. Teor. Fiz.* **32**, 232 (1980) [*JETP Lett.* **32**, 214, (1980)].
- ¹⁰³A. V. Deryagin, N. V. Kudrevatych, R. Z. Levitin, and Yu. F. Popov, *Phys. Status Solidi A* **51**, K125 (1979).
- ¹⁰⁴A. Miller, T. D'Silva, and H. Rodrigues, *IEEE Trans. Magn.*

- MAG-12, 1006 (1976).
- ¹⁰⁶K. P. Belov, O. P. Elyutin, G. I. Kataev, D. Kim, S. A. Nikitin, G. V. Pshechenkova, L. I. Solntseva, G. N. Surovaya, and V. P. Taratynov, *Fiz. Met. Metalloved.* **39**, 284 (1975).
- ¹⁰⁶V. I. Khrabrov and Ya. S. Shur, *Pis'ma Zh. Eksp. Teor. Fiz.* **20**, 468 (1974) [*JETP Lett.* **20**, 213 (1974)].
- ¹⁰⁷A. I. Mitsek, *Fiz. Tverd. Tela (Leningrad)* **5**, 1800 (1963) [*Sov. Phys. Solid State* **5**, 1312 (1964)].
- ¹⁰⁸R. R. Birss, *Symmetry and Magnetism*, North-Holland, Amsterdam, 1964.
- ¹⁰⁹N. C. Koon and C. M. Williams, *J. Appl. Phys.* **49**, 1948 (1978).
- ¹¹⁰N. C. Koon and C. M. Williams, *J. Phys. (Paris)* **40**, 94C (1979).
- ¹¹¹R. Street and S. Lewis, *Proc. Phys. Soc. London* **72**, 604 (1958).
- ¹¹²K. P. Belov, R. Z. Levitin, and S. A. Nikitin, *Usp. Fiz. Nauk* **82**, 449 (1964) [*Sov. Phys. Usp.* **7**, 179 (1964)].
- ¹¹³S. B. Palmer and E. W. Lee, in: *Trudy Mezhdunarodnoi konferentsii po magnetizmu (Proceedings of the International Conference on Magnetism) MKM-73*, Nauka, M., 1974, Vol. 1(2), p. 169.
- ¹¹⁴E. S. Fischer and D. Dever, *Trans. Met. Soc. AIME* **239**, 48 (1967).
- ¹¹⁵G. I. Kataev and V. V. Shubin, *Fiz. Met. Metalloved.* **48**, 188 (1979).
- ¹¹⁶H. T. Savage, A. E. Clark, and J. M. Powers, *IEEE Trans. Magn.* **MAG-11**, 1355 (1975).
- ¹¹⁷G. I. Kataev and V. V. Shubin, *Akust. Zh.* **26**, 142 (1980) [*Sov. Phys. Acoust.* **26**, 77 (1980)].
- ¹¹⁸A. E. Clark and H. T. Savage, *IEEE Trans. Sonics Ultrason.* **SU-22**, 50 (1980).
- ¹¹⁹B. S. Berry, W. C. Pritchett, and H. T. Savage, *J. Appl. Phys.* **49**, 6075 (1978).
- ¹²⁰V. F. Novikov, E. V. Dolgikh, A. I. Ul'yanov, and A. V. Deryagin, *Fiz. Met. Metalloved.* **48**, 1093 (1979).
- ¹²¹V. F. Novikov and E. V. Dolgikh, *ibid.* **51**, 980 (1981).
- ¹²²S. Butterworth and F. D. Smith, *Proc. Phys. Soc. London* **43**, 166 (1930).
- ¹²³A. A. Kharkevich, *Zh. Tekh. Fiz.* **12**, 331 (1943).
- ¹²⁴L. N. Syrkin, *Piezomagnitnaya keramika (Piezomagnetic Ceramics)*, L., 1972.
- ¹²⁵Z. Kaczkowski, *Materiay piezomagnetyczne i ich zastosowania (Piezomagnetic Materials and Their Applications)*, PAN, Warsaw, 1978.
- ¹²⁶E. Kikuchi, *Ul'trazvukovye preobrazovateli (Ultrasonic Transducers)*, Mir, M., 1972.
- ¹²⁷K. P. Belov, K. V. Epifanova, G. I. Kataev, L. I. Solntseva, and G. E. Chuprikov, *Nauchnye trudy GIREDMETA (Scientific Works of the State Research Institute for Rare Metals)*, Metallurgiya, M., 1976, Vol. 69, p. 104.
- ¹²⁸K. P. Belov, G. I. Kataev, S. A. Nikitin, and G. E. Chuprikov, *Akust. Zh.* **22**, 768 (1976) [*Sov. Phys. Acoust.* **22**, 431 (1976)].
- ¹²⁹A. E. Clark, J. R. Cullen, and K. Sato, *AIP Conf. Proc.* **24**, 670 (1975).
- ¹³⁰A. E. Clark, *ibid.* **18**, 1015 (1974).
- ¹³¹A. E. Clark, R. Abbundi, and W. R. Gilmor, *IEEE Trans. Magn.* **MAG-14**, 542 (1978).
- ¹³²A. F. Popkov, Abstract of candidate's dissertation, Moscow State University, M., 1977.
- ¹³³A. E. Clark, H. S. Belson, and N. Tamagawa, *Phys. Rev. Lett.* **42A**, 160 (1972).
- ¹³⁴M. Dariel and U. Atzmony, *Intern. J. Magnetism* **4**, 213 (1973).
- ¹³⁵C. M. Williams and N. C. Koon, *Physica (Utrecht) Ser. B* **86-88**, 147 (1977).
- ¹³⁶H. T. Savage and A. E. Clark, in: *Rare Earths and Actinides: Intern. Conference, Durham, 1977-Bristol*, London, 1978, p. 310.
- ¹³⁷R. Abbundi and A. E. Clark, *IEEE Trans. Magn.* **MAG-13**, 1519 (1977).
- ¹³⁸J. B. Milstein, N. C. Koon, L. R. Johnson, and C. M. Williams, *Mater. Res. Bull.* **9**, 1617 (1974).
- ¹³⁹K. P. Belov, É. P. Bochkarev, I. P. Golyamina, G. I. Kataev, I. N. Kuppenko, S. A. Nikitin, V. K. Chulkova, and G. E. Chuprikov, in: *Trudy IX Vsesoyuznoi akusticheskoi konferentsii (Proceedings of the 9th All-Union Acoustical Conference)*, M., 1977, p. 15.
- ¹⁴⁰R. W. Timme, *J. Acoust. Soc. Am.* **59**, 459 (1976).
- ¹⁴¹B. M. Ivakin, E. V. Karus, and O. L. Kuznetsov, *Akusticheskiĭ metod issledovaniya skvazhin (The Acoustical Method of Investigating Boreholes)*, Nauka, M., 1978.
- ¹⁴²H. T. Savage, R. Abbundi, A. E. Clark, and O. D. McMasters, *J. Appl. Phys.* **50**, 1674 (1979).
- ¹⁴³H. T. Savage, A. E. Clark, N. C. Koon, and C. M. Williams, *IEEE Trans. Magn.* **MAG-13**, 1517 (1977).
- ¹⁴⁴M. Malekzadeh, M. P. Dariel, and M. R. Pickus, *Mater. Res. Bull.* **11**, 1419 (1976).
- ¹⁴⁵R. C. Johnson, A. E. Miller, and B. G. Koepke, in: *Rare Earths Modern Science and Technology*, New York, London, 1978, p. 331 (Honeywell Corporate Materials Science Center, Bloomington, MN 55420).
- ¹⁴⁶M. Malekzadeh and M. R. Pickus, *Appl. Phys. Lett.* **33**, 108 (1978).
- ¹⁴⁷M. Malekzadeh and M. R. Pickus, *IEEE Trans. Magn.* **MAG-16**, 536 (1980).
- ¹⁴⁸S. W. Meeks and R. W. Timme, *J. Acoust. Soc. Am.* **62**, 1158 (1977).
- ¹⁴⁹J. L. Butler and S. J. Ciosek, *ibid.* **67**, 1809 (1980); S. M. Cohick and J. L. Butler, *ibid.* **72**, 313 (1982).
- ¹⁵⁰S. A. Nikitin, D. Kim, Yu. F. Popov, A. K. Zvezdin, and A. F. Popkov, *Fiz. Tverd. Tela (Leningrad)* **17**, 2659 (1975) [*Sov. Phys. Solid State* **17**, 1767 (1975)].
- ¹⁵¹D. Gignoux, D. Givord, F. Givord, and R. Lemaire, *J. Magn. Mater.* **10**, 288 (1979).
- ¹⁵²V. A. Domyshv, V. A. Buravikhin, and O. D. Glebova, in: *Fizika magnitnykh yavlenii (Physics of Magnetic Phenomena)*, Irkutsk, 1979, p. 3.
- ¹⁵³S. A. Nikitin, *Izv. Akad. Nauk SSSR Ser. Fiz.* **42**, 1707 (1978).
- ¹⁵⁴K. P. Belov, G. I. Kataev, and R. Z. Levitin, *Zh. Eksp. Teor. Fiz.* **37**, 938 (1959) [*Sov. Phys. JETP* **10**, 670 (1960)].
- ¹⁵⁵G. I. Kataev, *Fiz. Met. Metalloved.* **11**, 375 (1961).
- ¹⁵⁶D. C. Webb, K. L. Davis, N. C. Koon, and A. K. Ganduly, *Appl. Phys. Lett.* **31**, 245 (1977).

Translated by M. V. King